Physics – Uspekhi **38** (5) 497 – 521 (1995)

PACS numbers: 74.72.–h; 74.90.+n; 72.20.Dp; 75.50.Pp

Phase separation in high-temperature superconductors and related magnetic systems

E L Nagaev

Contents

Abstract. A review is given of theoretical and experimental data on spontaneous phase separation in nonsuperconducting degenerate magnetic semiconductors and related cuprate high-temperature superconductors. The following phenomena are considered: (1) The electronic phase separation occurring at frozen impurity positions as a result of charge carrier concentration in regions with a changed magnetic state; (2) impurity (chemical) phase separation when a nonuniform impurity distribution over a crystal is driven simultaneously by interaction between impurity atoms and by their tendency to concentrate inside regions with a changed magnetic ordering.

1. Introduction

The subject of the present review is the thermodynamic-equilibrium phase separation in conducting materials which include atoms with nonzero magnetic moment. Almost all high-temperature superconductors (HTSCs) and degenerate nonsuperconducting magnetic semiconductors belong to this class of materials. Strictly speaking, HTSCs discussed here should also be classified as degenerate magnetic semiconductors, though the role of the magnetic atoms in them is usually played not by transition or rare-earth metal atoms but by the copper atoms.

Phases into which these materials become separated differ in their electric, magnetic, and, in addition, very often in their chemical properties. The fact that the phase separation is observed both in superconducting and nonsuperconducting materials means that the immediate cause of the phase separation is not the superconductivity. On the other hand, superconductivity often occurs in the absence of phase separation, so one-to-one correspondence between them is nonexistent.

Nevertheless, one may believe that in some materials the phase separation creates optimum conditions for the appearance of superconductivity. As will be discussed below, it increases the charge carrier density in some regions, and, hence, the superconducting transition temperature, which increases with the carrier density for small values. In any case, the phase separation influences the properties of superconductors substantially. Discovered in many HTSCs (e.g., in La_2CuO_4-based materials, in yttrium ceramics and so on), phase separation became one of the main subjects of investigation in these materials.

The phase separation is by no means a monopoly of magnetic materials. However, this phenomenon is observed in them much more often than in nonmagnetic materials, which seems quite natural since a very effective additional channel for phase separation appears in them — the

E L Nagaev Institute of High Pressure Physics, Russian Academy of Sciences, 142092 Troitsk, Moscow Region, Russia
Fax (7-095) 334-00 12
E-mail: tsir@elch.chem.msu.su

Received 22 February 1994
Uspekhi Fizicheskikh Nauk **165** (5) 529 – 554 (1995)
Submitted in English by the author; edited by H Milligan

magnetic one. And in cases where nonmagnetic factors are the main cause of the phase separation, magnetic phenomena may aid them substantially. The present review is devoted to the description of various magnetic mechanisms of phase separation.

As is well known, semiconductors become degenerate as a result of their heavy doping with donor or acceptor impurities. At high impurity densities, delocalisation of the donor electrons or of the acceptor holes occurs, similar to the delocalisation of the external electrons of K-type or Na-type atoms when an alkaline metal is produced. As a result, what is virtually an impurity metal is produced inside a semiconducting crystal.

In using the term 'thermodynamic-equilibrium phase separation', one should keep in mind that two completely different situations exist. The first of them corresponds to a vanishingly small impurity atom diffusion when the impurity may be considered as frozen at all the actual temperatures. In this case one may only talk about thermodynamic equilibrium with respect to the charge carriers in the semiconductor.

The second case corresponds to the mobile impurity atoms which may be distributed over the crystal in thermodynamic equilibrium fashion. Then complete thermodynamic equilibrium takes place. Two different types of phase separation correspond to these two possibilities: the electronic one first predicted by the present author [1–4], and the impurity one discovered later.

Strictly speaking, the electronic phase separation may also occur in nondegenerate semiconductors which have an easily changeable phase state just like magnetic semiconductors. It consists in the formation by a charge carrier (a conduction electron, to be precise) of a region of a different, normally unstable phase. The region becomes stabilised by the electron localisation inside it. A necessary condition for this is that the electron energy in the changed phase should be substantially lower than in the initial phase.

The possibility of such a phenomenon, called heterophase charge carrier self-trapping, was first proved for an antiferromagnetic (AFM) semiconductor, inside which the conduction electron creates a region of ferromagnetic (FM) phase (the ferron state of a charge carrier [1, 2]). There are AFM semiconductors in which the energy difference between the AFM and FM states is very small. Then the FM region size found from the condition of minimum total energy for the system may be quite large. For example, in EuSe it may reach 10 000 atoms [5].

Heterophase electron self-trapping is also possible in regions of other phases. For example, if the initial structure of a semiconductor is staggered AFM, then the electron may be self-trapped inside it in a region of layered AFM or spin-disordered phase [6–8].

Whereas in nondegenerate semiconductors each electron is independent of other electrons, in degenerate semiconductors correlations between electrons are substantial. As a result, the electron self-trapping inside regions of changed phase becomes a cooperative phenomenon: in each region of changed phase there are many electrons simultaneously, and regions of initial and changed phases interacting with each other form a complicated geometric structure [3, 4, 9–13].

As all the electrons are concentrated in the regions with changed magnetic ordering (e.g., in FM ones inside the AFM semiconductor) but are absent from the initial AFM portion of the crystal, the FM and AFM portions have opposite charge. For this reason Coulomb forces arise in the crystal. They tend to intermix both phases. Thus, in the case considered the two phases are not independent and cannot be separated from each other, because they are connected in a united system by these forces. In this respect the universally accepted term 'phase separation' is inexact for the electronic version of the phase separation discussed here.

The Coulomb interaction, together with the surface interphase energy, also determines the topology of the two-phase state. At small enough electron densities the high-conducting FM portion of the crystal consists of noncontacting nanometer droplets inside the insulating AFM host. Consequently, the crystal as a whole behaves like an insulator. But, on increasing electron density, the droplets begin to make contact with each other. Thus, the percolation of the electron liquid and FM ordering occur simultaneously, resulting in an insulator–metal phase transition.

It should be stressed that the state just described is the ground state of a crystal and differs radically from the two-phase state at the first order phase transition. In essence, it is a specific state of solids resembling, to some extent, the Wigner crystal. The first experimental confirmation of the electronic phase separation in degenerate AFM semiconductors was obtained for EuSe and EuTe [14–19].

A similar magnetic mechanism of electronic phase separation may also exist in HTSCs. As an alternative to it, a lattice mechanism which may exist in materials with easily changeable lattice state may be indicated [20–22].

Turning to the impurity phase separation, one should keep in mind that usually the impurity is mobile only at quite high temperatures. In some important cases, in particular, in HTSCs, considerable impurity diffusion is observed up to 150–200 K. But impurity diffusion at still lower temperatures is possible if it occurs via quantum tunnelling or under illumination [23].

The impurity phase separation is driven by the interaction between impurity atoms and consists of the appearance of a nonuniform impurity distribution over the crystal which may occur without a change in the state of the host crystal. For this reason such a phase separation may also exist in the nonmagnetic degenerate semiconductors in which it was discovered for the first time (Si:Li, GeTe:Te [23–26]). As each phase at the impurity phase separation is electroneutral, such a phase separation is genuine. A theory for this effect based on the impurity metal concept was developed in Ref. [27].

Though there are no Coulomb forces at the impurity phase separation, nevertheless, here, too, physical reasons exist for phase intermixing being energetically favoured: this process reduces the elastic energy of the system [28, 29]. Certainly, the single-phase region size in this case is several orders of magnitude larger than at the electronic phase separation.

In magnetic crystals, both superconducting and nonsuperconducting, the impurity phase separation should have a specific character. On one hand, generally speaking, nonuniformity in the impurity distribution should lead to nonuniformity in the magnetic properties of a crystal. On the other hand, if change in the magnetic ordering reduces the impurity atom energy, it assists the impurity phase separation. In other words, it is driven by the interaction

between magnetic atoms and the tendency of magnetic atoms to change the magnetic ordering simultaneously. Unlike the electronic phase separation, at such a magneto-impurity phase separation a two-phase state (the AFM – FM or another) may exist in which both the phases are highly conducting (one of them or even both may be superconducting) [30].

2. The model and single-electron phase separation

2.1 The model

In what follows, both superconducting and nonsuperconducting materials will be treated from a unified point of view as magnetic conductors (more precisely, as semiconductors). It is generally accepted that properties of semiconducting rare-earth and transition metal compounds are adequately described in most cases by the $s-f$ (or, which is the same, by the $s-d$) model.

As for HTSCs and related compounds, usually one describes their properties with the aid of the Hubbard model in the limit of the on-site interaction $U \to \infty$ or the $t-J$ model which is very close to it. But in reality, for HTSCs, too, one may use the $s-d$ model generalised in such a manner as to take into account the Coulomb interaction between electrons and ionised impurities since it is more general than the models just mentioned. In particular, the $t-J$ model may be obtained as a particular case of the $s-d$ model (see below).

The Hamiltonian of the $s-d$ model is taken in the form

$$H = \sum E_k a^*_{k\sigma} a_{k\sigma} - \frac{A}{N_t} \sum \boldsymbol{S}_{\boldsymbol{h}} s_{\sigma\sigma'} \exp\left[i(\boldsymbol{k}-\boldsymbol{k}')\boldsymbol{g}\right] \times a^*_{k\sigma} a_{k'\sigma'} - \frac{1}{2}\sum I(\boldsymbol{g}-\boldsymbol{f})\, \boldsymbol{S}_{\boldsymbol{g}} \boldsymbol{S}_{\boldsymbol{f}} + H_C \,, \quad (1)$$

where $a^*_{k\sigma}$, $a_{k\sigma}$ are the creation and annihilation operators for an s-electron with quasimomentum $\boldsymbol{k}$ and spin projection σ, $\boldsymbol{S}_{\boldsymbol{g}}$ is the operator of the d-spin of the atom with number $\boldsymbol{g}$, $s_{\sigma\sigma'}$ are the Pauli matrices, N_t the total number of cells in the crystal. If the s-electron moves over the magnetic atoms the label $\boldsymbol{h}$ in the second term in (1) coincides with $\boldsymbol{g}$. But if it moves over nonmagnetic atoms (e.g., a hole over the oxygen ions) then $\boldsymbol{h}$ corresponds to the nearest magnetic neighbours of this atom, and summation is carried out over them. The term bilinear in the d-spin operators will be called the direct exchange Hamiltonian though in reality it corresponds rather to the superexchange between magnetic atoms. The term H_C describes the electrostatic interaction in the system of electrons and ionised donors or holes and acceptors.

The main parameters of the $s-d$ model are the s-band width $W = 2zt \propto 1/ma^2$ (m is the s-electron effective mass, a is the lattice constant, $\hbar = 1$), the $s-d$ exchange energy AS (S is the d-spin magnitude), the direct exchange energy zIS^2 which is of order of the magnetic ordering temperature T_N, and the electrostatic energy $e^2 n^{1/3}/\varepsilon$, where n is the s-electron density, ε the dielectric constant of the crystal, z the nearest neighbour number. As discussed in Ref. [9], for rare-earth compounds where states of the conduction electrons are really of the s-type, the inequality $AS \ll W$ is typical. But in transition-metal compounds the charge carriers may be in states of the d-type, and for this reason the opposite inequality should hold.

As for HTSCs, if they are of the n-type, then the conduction electrons in the Cu – O planes move over magnetic Cu^{++} ions: arrival of a conduction electron on such a ion means its conversion into a Cu^+ ion. But this does not necessarily mean that it is in the $3d^{10}$ state. The $3d^9 4s^1$ state may turn out to be more energetically favoured since the Bloch overlap integral t_s between $4s$-orbitals of neighbouring atoms exceeds the Bloch integral t_d between the $3d$-orbitals of these atoms. In a general case the hybridisation of these states should take place.

If the conduction electron is in a hybridised state predominantly of the d-type, then the inequality $W \ll AS$ should hold, but if the state is mainly of the s-type, then one may expect the opposite inequality to be valid. It counts in favour of a relatively weak exchange interaction between s-electrons and localised d-moments in which, experimentally, the holes destroy the AFM ordering much more strongly than conduction electrons (cf. e.g., Ref. [31]).

Now we proceed to holes. Principally, they also may move over Cu ions producing Cu^{3+} ions, and then the inequality $W \ll AS$ should hold. But generally it is believed that in reality they move over the oxygen ions. While not insisting on the universality of the first version, I would like only to indicate, that within the framework of the second version it is difficult to explain the experimental fact already mentioned according to which holes destroy the magnetic ordering much more strongly than electrons. Meanwhile, the exchange interaction between magnetic Cu ions and holes should be weaker than that between them and electrons since holes are spatially separated from these ions. For this reason I believe it is preferable to admit both these possibilities for holes, as well as the possibility of the inequality $W \gg AS$ for holes if they move over the oxygen ions.

Independently of the relationship between AS and W, both these quantities should greatly exceed zIS^2, as even for narrow d-bands these quantities are, respectively, of the zeroth, first, and second order in the overlap of nearest neighbour orbitals (generalisation to the superexchange is obvious).

All the numerical results presented below are obtained for the case $W \gg AS$. In this case the sign of A is not essential, and in what follows, for the sake of simplicity, the quantity A will be taken as positive. The inequalities

$$AS > \mu \gg \frac{e^2 n^{1/3}}{\varepsilon} \quad (2)$$

will be used, where μ is the Fermi energy. The first of them relates to a relatively small number of charge carriers in a degenerate semiconductor; the second inequality is the standard condition for a semiconductor to be degenerate.

Let us discuss the case $W \ll AS$ briefly. In this case results depend substantially on the sign of A, i.e. on the magnitude of the spin of the Cu^{3+} ion. According to Ref. [9], at $A < 0$ and $S = 1/2$ the Hamiltonian (1) reduces to the Hamiltonian of the $t-J$ model. The latter differs from the initial Hamiltonian (1) in the absence from it of a term $\sim A$ (this term reduces to an additive constant). But, if carriers are holes, eigenstates of the remaining part of the Hamiltonian should meet the condition that the number of electrons on each atom be less than 2.

Such a Hamiltonian may be used for some n-HTSCs. But I am not sure that it is applicable to p-HTSC, too. If the

hole moves over the oxygen ions then, as was already mentioned, the quantity A can hardly be very large. Directing our attention to the hypothetical case when the hole moves over the copper ions I must note that according to the Hund rule the magnitude of the Cu^{3+} spin should be equal to 1, i.e. it should correspond to $A > 0$. It might be zero only in a strong crystalline field of an appropriate symmetry. Meanwhile, properties of systems with small W, but with $s-d$ exchange integrals of different signs differ even qualitatively. So, results obtained for $W \gg AS$ are qualitatively valid for $W \ll AS$ only at $A > 0$ [9].

2.2 Single-electron and single-atom impurity phase separations

The main feature of magnetic semiconductors is a strong dependence of the electron energy on the magnetic ordering. To present this dependence in a rather general form, let us consider a structure intermediate between the FM and AFM — the canted two-sublattice structure with angle 2ϑ between the moments of sublattices and with the structure vector $\boldsymbol{Q}$. To simplify the treatment, the lattice will be assumed to be simple cubic or quadratic. Then in the second order in AS/W the electron energy is given by the expression following from Eqn (1) [31]

$$E_{k\sigma}^{t} = E_{k\sigma}^{c}(\boldsymbol{Q}) + E_{k\sigma}^{q} ,$$

$$E_{k\sigma}^{c}(\boldsymbol{Q}) = E_k - AS\sigma\cos\vartheta + \frac{A^2S^2\sin^2\vartheta}{4(E_k - E_{k+Q})} ,$$

$$E_{k\sigma}^{q} = \frac{1}{4}A^2S(1 - 2\sigma\cos\vartheta)\,G(E_k) ,$$

$$G(E) = \frac{1}{N}\sum(E - E_p - \mathrm{i}0)^{-1} . \qquad (3)$$

If the d-spins are completely disordered, the electron energy is given by the expression

$$E_k^{sl} = E_k + A^2S(S+1)\,G(E_k) . \qquad (4)$$

As follows from Eqns (3) and (4), the lowest electron energy is reached at the FM ordering, where it is in the main approximation $U_{FA} = AS/2$ lower than the energy of the AFM or disordered (spin liquid) state. But the energies of different AFM structures differ, too. For example, if one compares the minimum electron energies for the staggered Neel AFM ordering with $\boldsymbol{Q}_N = (\pi, \pi, \pi)$ and for the layered Landau ordering with $\boldsymbol{Q}_L = (\pi, 0, 0)$, one sees that the latter is lower than the former by the quantity $U_{LN} = E_{0\sigma}(\boldsymbol{Q}_N) - E_{0\sigma}(\boldsymbol{Q}_L) \propto A^2S^2/W$.

The same conclusion remains true also in the opposite limit $|A|S \gg W$. In this case in the nearest-neighbour approximation the electron energy difference between the FM and the staggered AFM ordering is given by expressions [1, 2, 9] which tend to $W/2$ at $S \Rightarrow \infty$ and diminish with S, vanishing for $S = 1/2$ at $A < 0$. The corresponding expressions for U_{LN} are rather complicated: proportional to W and sharply reducing with the d-spin magnitude S. At $S \Rightarrow \infty$ the quantity U_{LN} is equal to $W/6$ [13].

Though in degenerate semiconductors the phase separation is a cooperative phenomenon, it is advisable to begin with an 'elementary act' of phase separation — the heterophase self-trapping of a single electron in a non-degenerate semiconductor, which permits the elucidation of the physics of the phenomenon considered. Let us imagine that in the absence of the s-electrons the crystal is in a magnetic state with a high s-electron energy. Electrons tend to establish their low-energy magnetic state surmounting the direct exchange which determines the ordering in the insulating crystal. Certainly, a single electron cannot change the ordering in the entire crystal of macroscopic size. But it may do that inside a certain microregion. This region is a potential well for the electron of depth U. The radius R of the potential well should be found from the condition of the minimum total energy which is the sum of the electron energy inside the well and the direct-exchange energy used for rearrangement of the magnetic ordering in the corresponding region.

One easily obtains the following condition for this state to be energetically favoured [9, 13, 33]:

$$\frac{D}{W} \leqslant \frac{D_c}{W} = 0.2(4-d)\left(\frac{U}{W}\right)^{1+d/2} . \qquad (5)$$

Here D is the direct-exchange energy per magnetic atom used to create the region of the changed phase, d dimensionality of the space (at $d = 2$ the lattice is assumed to be simple quadratic). Eqn (5) is obtained in the nearest neighbour approximation for conduction electrons with $W = 12|t|$. The accuracy of the model used, in which a sharp boundary between two phases was assumed, was confirmed by a special investigation in Ref. [32].

For large radii R one may obtain an explicit expression for the energy and radius of the self-trapped electron in the 3-D case [1, 2]:

$$E = -U + \frac{5}{3}|\pi B|^{5/3}D^{2/5} , \qquad R = a\left|\frac{\pi B}{2D}\right|^{1/5} , \qquad (6)$$

where a is the lattice constant. In the 2-D case [33]

$$E = E_c(R) + \frac{\pi R^2 D}{a^2} , \qquad R = 0.63\left(\frac{W}{D}\right)^{1/4} a , \qquad (7)$$

where E_c is the lowest electron level in a circle-shaped potential well of depth U.

If an electron is captured by an impurity atom, it can change the magnetic ordering in its vicinity [2, 9]. As a result, in addition to the electrostatic impurity atom potential, an effective attraction potential acts upon the electron. It corresponds to the changed magnetic phase centred at the impurity atom. Thus, interaction of the electron with the magnetic subsystem reduces the captured electron orbit radius. This phenomenon may be called the single-atomic impurity phase separation.

2.3 Ferromagnetic regions in an antiferromagnet

Eqn (6) was obtained in the pioneering papers on heterophase self-trapping [1, 2] where the idea of electron self-trapping in the FM region inside the AFM semiconductor was advanced. In these papers the term magnetic polaron was used for such a quasiparticle, but in Ref. [34] I proposed the term ferron as more convenient for this quasiparticle. The results (6) were repeated by many authors (e.g. Ref. [35]).

If the AFM system is Heisenbergian or Isingian, then in the nearest-neighbour approximation $D = 6|I|S^2$, i.e., D is the quantity of the order of the Neel point T_N. Thus, one might expect that ferrons can exist only in low-temperature AFM systems. Nevertheless, there are AFM systems in which $D \ll T_N$. These are systems with the exchange interaction between more remote neighbours or of a higher order in spins.

For example, the isotropic metamagnetic system EuSe with $T_N = 4.6$ K, i.e. about 5×10^{-3} eV, which possesses a very complicated phase diagram (e.g., Ref. [9]), requires only $D \propto 10^{-5}$ eV to become FM. An order of magnitude lower energy is necessary to convert this antiferromagnet into a ferromagnet. In this case the size of the ferrimagnetic region should be $10a$, i.e. including several thousand atoms, and it should be surrounded by a ferrimagnetic layer. Remembering that the spin of the Eu^{++} atom is 7/2, one sees that the conduction electron induces in EuSe a moment four orders of magnitude greater than its own spin [5].

If the ferron exists in the absence of the external magnetic field H, it will be destroyed by the field, the strength of which exceeds the critical value $H_c = 2D(1 - 25D^2W^3/U^5)$ [9] . The ferron may be destroyed by heating, too. Nevertheless, it may remain stable up to quite high temperatures, even exceeding T_N. In the latter case one may speak of the ferron states in the paramagnetic (PM) crystal. At finite temperatures the quantity D in Eqn (5) is determined as the difference between the free energy of the FM ordering and the free energy of the AFM $(T < T_N)$ or PM $(T > T_N)$ state per atom. In the latter case

$$D(T) = T\ln(2S + 1) + \frac{I^2(S+1)^2}{24T} - 3IS^2 . \qquad (8)$$

Equating $D(T)$ to D_c (5), one obtains the ferron destruction temperature.

As follows from Eqns (4)–(6), the ferron in the 2-D case is considerably more stable than in the 3-D case. According to Eqn (5) the critical value of the direct exchange expenditure D_c in the 2-D case is $(3/2)(2W/AS)^{1/2}$ times higher than in the 3-D case. Respectively, the destruction temperature of the 2-D ferrons at the same W, AS, and D is several times higher (see Ref. [33]).

In an ideal crystal at $T = 0$ the ferron must move as a whole because of its translational invariance. But its band should be extremely narrow decreasing exponentially with increasing ferron radius [8]. (The same type of ferron energy dependence on R was pointed out in Ref. [36] in the opposite limit $W \ll AS$ without presenting calculations). Thus, the ferron effective mass should be of the order of the atomic mass which makes the scenario of the band motion unrealistic [8]. Taking into account the fact that real crystals are imperfect, and that a very low degree of imperfection is required to cause the Anderson localisation of a quasiparticle with a giant effective mass, one should conclude that the motion of the ferron in the crystal should occur via random walks. Such phonon-assisted ferron random walks are considered in Ref. [8].

The stability of the ferrons is enhanced due to polaronic effects which may be strong enough because magnetic semiconductors are the polar crystals. As is well known, a localised electron polarises the ionic lattice much more strongly than a delocalised one. Thus, polaronic effects strongly favour magnetic self-trapping, allowing ferron existence in antiferromagnets with D twice as high as in nonpolar crystals [37, 38]. In some cases (e.g., EuSe) the direct exchange integral is very sensitive to the external pressure, i.e. to the lattice parameter. The theory of ferrons in such materials is developed in Ref. [39].

In Ref. [2] ferrons bound to impurities were treated for the first time, too. Strictly speaking, each electron captured by an impurity must produce a magnetic moment in its vicinity. Under favourable conditions, close to the impurity atom an FM region, enveloped in a region of canted spins, should appear. Formation of bound ferrons may be considered as the single-atom impurity phase separation.

Strictly speaking, long-range AFM ordering is not a necessary condition for ferron existence: they may arise in other nonmagnetised or weakly magnetised materials. In particular, they may exist in materials with short-range AFM ordering, e.g., in spin glasses [40], as well as in ferrimagnets [41].

Experimental data confirming the existence of free ferrons in EuTe and EuSe are analysed in detail in Ref. [9]. In Ref. [9] numerous experimental data are also presented confirming the existence of bound ferrons in various AFM semiconductors. A very large review of the theoretical literature on ferrons published in 1970s – 1980s is presented in Refs [9, 12].

The discovery of HTSCs renewed interest in ferrons. They were rediscovered in many theoretical papers, e.g. Refs [36, 42–46], and pairing of the ferrons was suggested as a possible mechanism of high-temperature superconductivity. But, apparently, this is not the case, since the mobility of the ferrons is too low for this: it should be comparable with the mobility of ions, and for such classical systems an essentially quantum phenomenon such as superconductivity is impossible. The interest in bound ferrons (magnetic polarons) is related to the destruction of the long-range AFM order by dopants with the approach to the superconducting state [47, 48].

2.4 Regions of a changed phase in frustrated antiferromagnetic and magnetoexcitonic systems

In cases when ferrons are impossible other quasiparticles corresponding to the heterophase self-trapping may exist. First of all, the possibility will be discussed of electron self-trapping in an AFM semiconductor when another type of the AFM ordering is established in the localisation region. The electron energy in this phase should be lower than in the initial phase. An example was already given in the preceding section: the initial phase is the staggered AFM one, and the localisation phase is the layered AFM one. An additional gain in the energy of the self-trapped state may be obtained if one allows canting of the sublattice moments in the localisation region.

Such a quasiparticle, called an afmon [6, 7, 13], is especially energetically favoured if in the space of the direct exchange integrals between the n-nearest neighbours I_n the undoped crystal is close to the boundary between these phases. In the 3-D case, in addition to the phases with $\boldsymbol{Q} = (\pi, \pi, \pi)$ and $(\pi, 0, 0)$, the AFM phase with $\boldsymbol{Q} = (\pi, \pi, 0)$ is possible. If one assumes that $I_1 > 4I_3$, the latter can be excluded from the consideration as energetically unfavoured.

The situation described above exists at $2I_2 > I_1$ $(I_n < 0)$. Putting $D = 4(2I_2 - I_1)S^2$ and using a variational procedure with the following variational parameters: the canting angle ϑ and size L of the Landau region (assumed cubic or squared in the 3-D and 2-D cases, respectively), one obtains for $D \Rightarrow 0$ with allowance for Eqn (3): $\cos\vartheta \propto D^{d/d+2}$, $L \propto D^{-1/d+2}$. The latter estimate agrees with Eqn (5).

The reason for the size divergence at $D \Rightarrow 0$ is obvious. Disappearance of canting under the same condition is a consequence of the fact that, with increasing L, the electron

density per magnetic atom reduces. Hence, the molecular field of the electron acting upon spins of magnetic atoms reduces, too. Nevertheless, the total afmon moment remains finite at $D \Rightarrow 0$, though, unlike the ferron moment at $D \Rightarrow 0$, it does not diverge.

The case $AS \ll W$ considered above is not the most favourable for existence of the afmon. At large d-spins the opposite case seems much more favourable (at W and D fixed). At small spins the case $W \propto AS$ should be optimum. In this case U_{LN} may be quite comparable with U_{FA}. Meanwhile, limitations on D values are not very restrictive for the afmons. As follows from Eqn (4), they may even amount to a quantity comparable with T_N at realistic parameters, i.e. the system may be far from the phase boundary [13]. There are attempts to explain some experimental data in terms of the afmons [49].

As an alternative to the afmon, electron self-trapping inside a fully spin-disordered region may be considered [13]. Conditions for such a self-trapping are especially favoured in the 2-D case, when, in the Born approximation, the $s-d$ shift (4) of the s-electron energy in the disordered region diverges logarithmically at the bottom of the conduction band. But this energy shift in the AFM state should be much less (at fixed AS and $S \Rightarrow \infty$ it remains finite). For this reason the disordered region is a potential well for the conduction electron in an antiferromagnet though the electron level inside it is spread out due to spin fluctuations. Certainly, its depth should be less than for the FM region. But, on the other hand, the $d-d$ exchange energy expenditure for creation of an FM ordering in a region should be considerably larger than for its magnetic disordering. For this reason it may turn out that the self-trapping inside a disordered (spin-liquid) region is more energetically favoured than inside an FM region or inside a region of another AFM phase. The requirement that the system should be frustrated is not essential here. The energy of the quasiparticle may be further reduced if it acquires a small magnetic moment.

One may also point out some other possible types of magnetic heterophase self-trapping. But they cannot be obtained within the framework of the standard $s-d$ model. In this model (1) only the intraband $s-d$ exchange integral A is taken into account since the interband $s-d$ exchange integral connecting the states of the conduction and valence bands is normally small compared with A. But if occasionally the opposite inequality holds then the electron energy in the AFM state turns out to be lower than in the FM state. For this reason the electron tends to become self-trapped inside an AFM region arising in the FM semiconductor. Such a quasiparticle was named the antiferron [50]. Though such a situation seems rather exotic, nevertheless, some FM semiconductors with anomalous properties exist (e.g. $CdCr_2Se_xS_{1-x}$ [9]) in which antiferrons possibly exist [51].

Further, in some materials d-ions or f-ions entering them are diamagnetic but a very small energy (~ 0.01 eV) is required to make them paramagnetic. As an example, Co compounds may be mentioned [9]. In such materials the conduction electron may create a ferromagnetic region by causing the singlet-to-triplet transition in a group of ions by its localisation inside this group [52]. Unlike the ferrons in antiferromagnets, the depth of the arising potential well is $AS/2$ independently of AS/W. Thus, it may be much deeper than in an antiferromagnet. For this reason the stability of the ferron in a diamagnetic crystal may be very large.

Certainly, even if the magnetic ion possesses an initial magnetic moment, it may be changed by the conduction electron, or a change in the orbital state of the localised d-electrons may occur leading to enhancement of the $s-d$ exchange. This may lead to the formation of ferron-like states, too. Singlet magnetic systems also provide favourable conditions for formation of such states [53, 54]

3. Cooperative phase separation

3.1 A general physical picture

In this section phase separation is considered in a degenerate semiconductor with frozen positions of impurity atoms ('electronic phase separation'). Certainly, heterophase electron self-trapping is possible in degenerate semiconductors, too. But in them the conduction electron density is so high that the electrons cannot behave independently of each other. Thus, there is no reason to believe that each electron becomes self-trapped independently: the self-trapping in degenerate semiconductors is a cooperative phenomenon [3, 4].

The tendency towards cooperative self-trapping is caused by the fact that if several electrons are located in the same region of the changed phase, the direct exchange energy required for its creation is less than for the creation of a separate region for each electron. But, on the other hand, concentration of many electrons in the same region causes the appearance of charge separation in the crystal since the depleted regions become charged oppositely to electron-rich regions. This increases the Coulomb energy of the system.

Certainly, to diminish the Coulomb energy, both the phases should be intermixed. Otherwise, the Coulomb energy per electron λ_C would be macroscopically large:

$$\lambda_C \propto \frac{e^2 n^{1/3}}{\varepsilon}\left(\frac{L}{a}\right)^{2/3}, \tag{9}$$

where ε is the dielectric constant, a the lattice constant, n the electron density, L the size of the crystal. But, on the other hand, if the electron-rich regions are too small, the electron kinetic energy increases sharply due to the spatial quantisation. Thus, the detailed structure of the cooperative self-trapped state should be found taking into account all these factors.

It is necessary to stress that the term 'phase separation' is not quite accurate in the case considered, since both phases into which the crystal is divided are united by the Coulomb forces and cannot be separated from each other. On the other hand, these forces determine the detailed structure of the phase-separated state and its electric properties. Ultimately, they may make the phase-separated state energetically unfavoured. This shows that the Coulomb forces play a fundamentally important part in the electronic phase separation.

In discussing the ground state of a phase-separated degenerate semiconductor, one may start from a degenerate semiconductor with relatively low electron density at $T = 0$. In it single-electron ferrons (or afmons etc) are possible. Let us discuss first the AFM–FM phase separation. On increase in the average electron density, the number of electrons in each FM region increases, as well as the size of

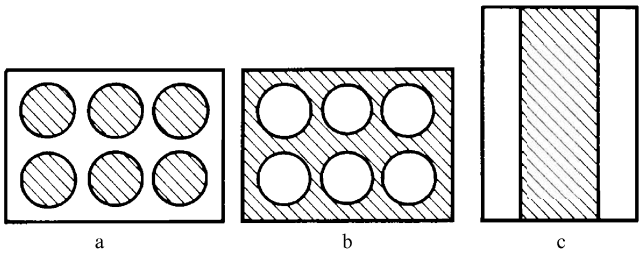

Figure 1. Two-phase states of a degenerate antiferromagnetic semiconductor: (a) insulating state of a bulk sample, (b) conducting state of a bulk sample, (c) layered state of a thin film (hatched is the ferromagnetic part and nonhatched the antiferromagnetic part of the crystal) [4, 10].

such regions. If one neglects the fluctuations of the impurity electrostatic potential, then the highly-conductive FM regions (droplets) should form a periodic structure inside the insulating AFM host (Fig. 1a). Such a structure resembles the Wigner crystal but, unlike it, here at each site not one but several electrons are located, and the magnetic ordering at the sites differs from the ordering in the rest of the crystal. On the other hand, this structure corresponds to superposition of strongly nonlinear charge and spin density waves.

Due to the impurity potential the droplet lattice discussed is not ideally periodic. These droplets are pinned and cannot move freely throughout the crystal. On the other hand, as the droplets are separated from each other by insulating AFM regions, the electrons cannot go over from one droplet to another. Thus, the degenerate semiconductor behaves like an insulator.

Starting from a certain critical density n_p, the FM droplets begin to make contact with each other. From this instant ('percolation threshold') the two-phase state becomes conducting. It corresponds to AFM insulating droplets inside the highly-conductive FM host (Fig. 1b). In other words, at n_p a change in the topology of the FM portion of the crystal takes place: it converts from a multiply-connected region to a simply-connected region. This transformation corresponds to the concentration phase transition from the nonconducting state to the conducting state occurring at $T = 0$. A similar transition may be caused by a magnetic field or by a rise in temperature.

In the case of thin films where an important part is played by the repulsive or attractive surface potential, a layered structure of the two-phase state with alternating conducting FM and insulating AFM layers may turn out to be more energetically favoured than the structure described above [10]. In such a geometry the film is always conducting along its plane and insulating across it (Fig. 1c).

The two-phase state may be destroyed by an external magnetic field or by a rise in temperature. In the first case the crystal goes over to the single-phase FM state, in the second case to the paramagnetic (PM) state. If the initial AFM–FM state was insulating, this means existence in the system under consideration of metal-insulator transitions induced by a rise in temperature or by a magnetic field.

The situation in the case of the staggered AFM-layered AFM phase separation differs from the described above in that the canting of the sublattice moments should depend on the electron density. To illustrate this, one should note that in an afmon of a sufficiently large radius the canting is nonzero. But in a biafmon it vanishes since both its electrons tend to occupy the same orbital level, i.e., to have opposite spins [13, 55]. In a general case the canting may be found only by a numerical calculation. A small magnetisation may exist also at the phase separation into the staggered AFM and spin-liquid phases.

By the way, the competition between the self-trapping inside the FM or the spin-liquid phase mentioned in Section 2.4 has much more chances to be won by the spin liquid here than in the case of a single electron. In fact, if magnetisation of the spin liquid is weak or nonexistent, then the electron kinetic energy must be lower in it than in an FM region where an orbital state cannot be occupied by two electrons with opposite spins

After the appearance of papers [3, 4], numerous papers were published in which instability of the uniform state of an AFM semiconductor was found without taking into account the Coulomb forces (e.g., Refs [56, 57]). But such a model cannot prove the possibility of the phase separation for real magnetic semiconductors. Moreover, it cannot reproduce their properties. Perhaps, possibly, results [56, 57] may be applied to the FM-AFM state of the ^{3}He crystals in which vacancies should concentrate in the FM portion of the crystal [58–61].

In some papers (e.g., Refs [62–65]) results of Refs [3, 4] are taken as a basis for further investigations. There are also papers in which a much simpler phenomenon — formation of biferrons — was investigated (e.g., Ref. [66]). A new rise of interest in the theory of phase separation occurred after the discovery of HTSCs. The corresponding papers will be discussed in Section 5.3.

3.2 The calculating procedure and two-phase states at $T = 0$

Here a computational procedure will be described for the AFM–FM state of a degenerate AFM semiconductor [10]. This procedure which permits the investigation of phase transitions in such a system at finite temperatures and melting of the nonuniform state is a direct generalisation of the procedure [3, 4] for the case of finite temperatures. The calculation is carried out with the aid of a variational procedure for the free energy of the system which takes into account the fact that the magnetisation of regions where the *s*-electrons are concentrated differs from its maximum value. Respectively, in no-electron regions the AFM order at finite temperatures is partially or completely destroyed (strictly speaking, at finite temperatures the conduction electrons must be present in these regions, too, but their number is exponentially small). These regions may be magnetised by an external magnetic field, the presence of which is taken into account in the calculation. The ratio x of the volume of these regions to the volume of the FM regions is the first variational parameter. The geometry of the phase-separated state corresponds to Fig. 1a or 1b. The radius R of a spherical minority phase inclusion is the second variational parameter.

The total free energy of the system is given by the expression

$$F = E_V + E_S + E_C + F_M \ . \tag{10}$$

Here E_V and E_S are, respectively, the bulk and surface energy of the electron gas. Account is taken of the fact that, due to the degeneracy of the electron gas, contribution of the thermal excitations to its free energy can be

neglected. Separation of the electron energy into the bulk and surface parts corresponds to the Born–Oppenheimer approximation and is carried out by introducing the coarse-grained density of states $g(E)$ in full analogy with calculations for small metal particles [67]:

$$g(E) = \pi^{-2} m^{3/2} \left(\frac{E}{2}\right)^{1/2} V \left[1 - \frac{\pi S}{4(2mE)^{1/2} V}\right], \qquad (11)$$

where V and S are the volume of the FM phase and the area of the AFM–FM interphase surface. In writing Eqn (11) the complete spin polarisation of the conduction electrons is taken into account.

Using Eqn (11), one obtains for a crystal of unit volume:

$$E_V = \frac{3}{5} \mu_f(n)\, n (1+x)^{2/3}, \quad \mu_f = \frac{(6\pi^2 n)^{2/3}}{2m}. \qquad (12)$$

The surface energy corresponds to electron wave functions vanishing on the boundary between the FM and AFM phases:

$$E_S = \frac{5}{16} \left(\frac{\pi}{6}\right)^{1/3} \beta \frac{E_V}{n^{1/3}(1+x)^{1/3} R}, \qquad (13)$$

with $\beta = 3$ for the case of droplets occupied by the conduction electrons and $\beta = 3x$ for the case of empty spheres.

The Coulomb energy E_C is found by separation of the crystal into Wigner cells (each charged sphere is surrounded by a layer with total charge of the same magnitude but of the opposite sign):

$$E_C = \frac{2\pi n^2 e^2 R^2 f(x)}{\varepsilon}; \qquad (14)$$

$$f(x) = 2x + 3 - 3(1+x)^{2/3} \quad \text{for occupied spheres},$$

$$f(x) = x\left[3x + 2 - 3x^{1/3}(1+x)^{2/3}\right] \quad \text{for empty spheres}.$$

The free energy of the magnetic subsystem F_M is calculated in the mean-field approximation. One takes into account the fact that in the first order in AS/W an effective 'magnetic field' $H_e = Ana^3(1+x)/2$ caused by the $s-d$ exchange acts upon the d-spins in the phase occupied by electrons. As before, it is assumed that the electrons in the FM phase are completely spin-polarised. Then F_M is given by the sum of contributions from the more strongly and more weakly magnetised phases:

$$F_M = \frac{x}{1+x} F_M(H, T) + \frac{1}{1+x} F_M(H + H_e, T); \qquad (15)$$

$$a^3 F_M = -\frac{H^2}{4K} + KS_1^2 - TL\left(\frac{KS_1}{T}\right) \quad \text{at} \quad H \leqslant 2KS_1,$$

$$a^3 F_M = -\frac{KS_2^2}{2} - TL\left(\frac{H - KS_2}{T}\right) \quad \text{at} \quad H \geqslant 2KS_1,$$

where in the nearest neighbour approximation $K = -zI$, and

$$L(y) = \ln \sum_{m=-S}^{S} \exp\{my\}.$$

The mean spins S_1 and S_2 satisfy the following equations of self-consistency:

$$S_1 = SB_S\left(\frac{SKS_1}{T}\right),$$

$$S_2 = SB_S\left[S\left(\frac{H - KS_2}{T}\right)\right], \qquad (16)$$

where B_S is the Brillouin function. Two different expressions for F_M in Eqn (15) correspond to the canted ordering and to the spin–flop phase.

In minimising the total free energy F with respect to R one should keep in mind that at $x > 1$ the geometry of Fig. 1a applies and at $x < 1$ the geometry of Fig. 1b applies. In all the cases only the Coulomb energy and electron surface energy are R-dependent, the former diminishing and the latter increasing, on decrease in R. This makes it possible to optimise expressions (13) and (14) with respect to R analytically, after which optimisation with respect to x is carried out numerically.

Calculations of the two-phase staggered AFM–layered AFM state follow the same pattern but they are more complicated because of the presence of a third variational parameter—the angle ϑ determining the canting of the sublattice moments in the regions where the conduction electrons are concentrated [13, 55].

Numerical calculations of the FM–AFM state were carried out for the following values of parameters corresponding to rare-earth compounds of EuTe type: $S = 7/2$, $JS^2 = 0.001$ eV (this corresponds to $T_N = 5$ K), $AS = 1$ eV, $\varepsilon = 20$, $a^{-3} = 4 \times 10^{22}$ cm^{-3}; and the effective mass equal to the free electron mass. The numerical results for the ground state of a bulk sample are as follows. The electron percolation density n_p at which a transition occurs from the two-phase insulating state to a two-phase conducting state is equal to 1.05×10^{20} cm^{-3}. Such a density is typical of degenerate semiconductors which confirms the reality of the phenomenon under investigation. The corresponding values of the FM droplet radius and the number of electrons in the droplet are: $R = 3.14$ nm, $N_d = 28$, which justifies the many-electron approach adopted above. The maximum gain in energy caused by the phase separation amounts to 0.15 eV per s-electron (the single-phase state is considered to be collinear AFM, canted two-sublattice or collinear FM, depending on the electron concentration).

In the case of the two-phase AFM–AFM state the same values of the electron parameters and the following parameters of the direct exchange interaction are taken: $l = (2I_2 - I_1)S^2 = 5 \times 10^{-4}$ eV, $k = -(6I_1 + 8I_2)S^2 = 0.01$ eV. Then one obtains the percolation parameters: $n_p = 1.3 \times 10^{20}$ cm^{-3}, $R = 2$ nm and $N_d = 8$. The canting is absent for such parameters. But if one reduces k by half with the other parameters unchanged, the canting appears: $\cos\vartheta = 0.097$. At $k = 0.001$ eV the AFM–FM state discussed above becomes more energetically favoured than the AFM–AFM state. The tendency toward increase in the magnetisation of the electron droplets with reducing k was observed for other parameters, too.

3.3 Phase diagrams at phase separation

The FM–AFM state under discussion is very sensitive to external magnetic fields and to increase in temperature. Various phase transitions are possible in such a state. They

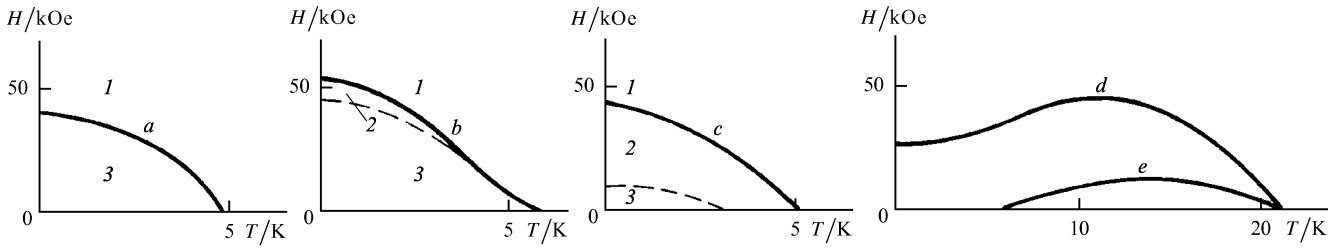

Figure 2. Phase diagrams for different values of the electron concentration. For a bulk sample $n = 10^{19}$ cm^{-3} (curve *a*); $n = 5 \times 10^{19}$ cm^{-3} (curve *b*); $n = 10^{20}$ cm^{-3} (curve *c*) [10]. For a 5 nm-thick film $n = 2 \times 10^{20}$ (curve *d*) and 3.5×10^{20} cm^{-3} (curve *e*). Solid linescorrespond to boundaries between uniform and nonunifom states, dashed lines to boundaries between conducting and insulating two-phase states [10].

may be illustrated by results of numerical calculations [10] mentioned above. The following values of the electron density, all of which are smaller than n_p, will be considered: 10^{19}, 5×10^{19}, and 10^{20} cm^{-3}. These results are shown in Fig. 2 (curves *a, b,* and *c*) in the form of phase diagrams in the $T-H$ plane. Here areas *1, 2, 3* denote regions of absolute stability for the uniform state, the two-phase conducting state, and the two-phase insulating states, respectively. Obviously, the uniform state should be conducting since the electron liquid is not localised inside droplets and is distributed over the entire crystal.

It is clear from Fig. 2 (curve *a*) that, on increase in T and H, for sufficiently small electron densities only a transition from the two-phase insulating state to the uniform conducting state is possible. In contrast to the crystal-to-liquid transition, this transition, even in the self-consistent field approximation, is found to be discontinuous with regard to the magnetic structure of the crystal and the spatial distribution of electrons.

In the region where the two-phase insulating state is stable, the parameters of this state change in the following way as T and H increase: the radius of the electron spheres and the number of electrons within the sphere increase, while the density of these spheres and the value of x decrease.

At sufficiently high electron density, three states can be stable within the framework of the approximations used here: the uniform phase, the conducting two-phase state, and the insulating two-phase state (see Fig. 2, curves *b, c*). Accordingly, as temperature changes, the class of phase transitions that are possible in such a system is enlarged: along with transitions from the heterophase to the uniform state, phase transitions between the heterophase conducting and heterophase insulating states may happen.

At an electron density of 5×10^{19} cm^{-3} corresponding to Fig. 2 (curve *b*) such transitions occur only in a magnetic field, while for the density of 10^{20} cm^{-3} corresponding to Fig. 2 (curve *c*) they can occur in its absence. This implies that if the crystal is found in the heterophase insulating state at $T = 0$, then as the temperature increases it enters first the heterophase conducting state, i.e., an insulator–metal transition occurs. After this a first order transition to the uniform state occurs. Thus, here a new type of percolation exists: if normally it occurs with increasing concentration of the percolating substance, in the case considered the percolation is induced by the magnetic field or temperature rise.

As for transitions between the insulating and conducting heterophase states (the dashed curves in Fig. 2 correspond to these transitions), it is unfortunate that the geometries adopted here (spheres of one phase within a host of the other phase), although completely satisfactory far from the transition point, do not allow us to describe the heterophase state exactly near the transition point: there its geometry is much more complicated. Meanwhile, the geometries of Fig. 1a and Fig. 1b correspond formally to two different branches of the free energy (10), since for these branches the expressions for E_C (14) and E_S (13) are different. As a consequence, the transition from insulating to conducting heterophase states, while formally of first order, is in fact close to second order. Actually, the jumps in the parameters are not large: the parameter x changes at n_p only by 20%.

It is natural to assume that the geometry of Fig. 1a in fact evolves continuously into the geometry of Fig. 1b. Then the two-phase state would correspond to a single branch of the free energy. If the phase transition is in fact a second-order transition, then it differs from the usual type of the transition in the absence of an increase in the symmetry of the system at the transition point. Thus, it cannot be described by the Landau theory. A phenomenological theory of such non-Landauian second-order phase transitions is proposed in Ref. [11] and developed further in Ref. [68].

Consider now the case when the density of the electrons is more than n_p but less than the density $n_u = 1.9 \times 10^{20}$ at which the phase separation disappears at $T = H = 0$. Then at zero temperature and external magnetic field the system is in a conducting heterophase state. As the temperature or field increases, this state passes into the uniform state through a first-order phase transition. If $n > n_u$, then the system is always found in the uniform state for any T and H.

A similar investigation of thin films with the geometry of Fig. 1c shows that the only possible type of phase transition in them is the second order phase transition from the two-phase state into the uniform state, when, on increase in temperature, the thickness of the surface AFM layers goes to zero continuously. At some values of parameters the ground state of the system may be uniform but, on increase in temperature, the reentrant phase transition is possible: first from the uniform state to the two-phase state and then the reverse transition (Fig. 2, curves *d, e*) [10].

Phase transitions in two-phase AFM–AFM or AFM–spin liquid systems should be of the same type [13, 55] but detailed numerical calculations are not available at present.

3.4 Experimental data (magnetic and magneto-optical investigations)

Experimental data on degenerate EuSe and EuTe give a very impressive confirmation of the AFM–FM phase separation in them, supporting the theory [3, 4, 10]. Unfortunately, direct neutronographic investigations of these materials are hampered by a very strong neutron absorption by Eu atoms. In addition, droplets of the nanometer size predicted by the theory (Section 3.2) may be not discovered by neutron scattering. But magnetic, optical, and electric measurements are quite convincing.

The magnetic data provide proof of coexistence of the AFM and FM phases at low temperatures. The presence of the AFM phase is established on the grounds of a magnetic susceptibility peak χ in very weak fields at the Neel point typical of the AFM systems. It is very important that the Neel point is the same as in an undoped crystal [14–17], this being proof that there are no conduction electrons in the AFM portion of the crystal (otherwise they would lower T_N because of indirect exchange via them).

Fig. 3 depicts the susceptibility $\chi(T)$ of a stoichiometric EuSe specimen and a nonstoichiometric one containing an excess of Eu [18]. They all display a peak at $T_N = 4.6$ K (the peak of χ in a stoichiometric specimen at 2.8 K is associated with a low-temperature phase transition absent from imperfect samples and has nothing to do with the phenomenon being discussed). EuTe doped with I behaves similarly [16, 17]. Doping with I also does not change the value of $\chi(H)$ at a fixed temperature, provided the field is not too low (where χ is H-independent, Fig. 4 [15]). This means that a doped crystal contains regions of the AFM phase with precisely the same properties as in an undoped crystal.

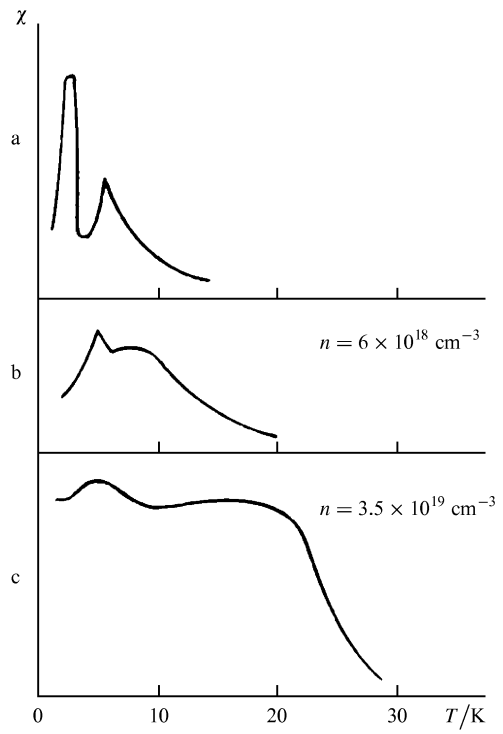

Figure 3. Initial magnetic susceptibility χ vs T of a stoichiometric (curve a) and nonstoichiometric (with excess of Eu) specimens of EuSe (curves b, c) with conduction electron concentrations at 300 K presented in Ref. [18].

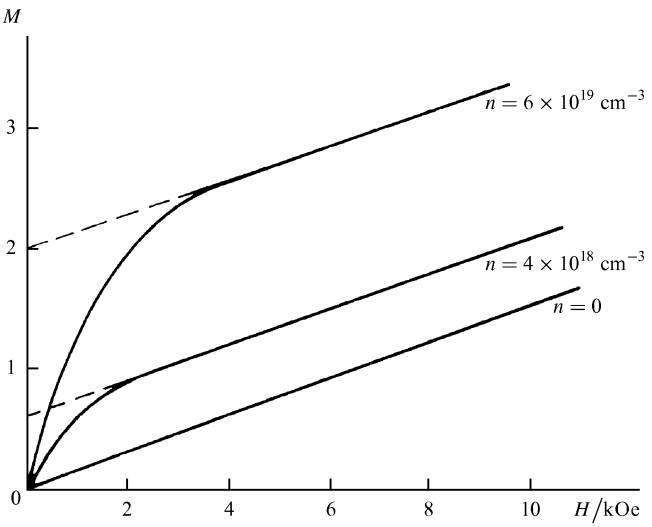

Figure 4. Magnetisation M vs. field H at 8 K for an undoped and an iodine-doped EuTe specimen with high-temperature conduction electron concentrations presented in Ref. [15].

The presence of the FM phase is proved by the behaviour of the magnetisation M of doped samples in weak fields which differs radically from the behaviour of undoped specimens. The former exhibit a sharp rise in magnetisation, the magnitude of which grows with the electron density n. The rise in the magnetisation of EuTe in fields of the order of 100 Oe, too small to change the angle between the sublattice moments of the antiferromagnet noticeably, can be explained only as a result of the aligning by the field of 'ready-made' magnetic moments of a large enough magnitude.

Judging by the fact that the linear dependence of M on H at 4.2 K starts in low fields of the order of 1 kOe (Fig. 4), the contribution of 'ready-made' moments already attains saturation in such fields. This means that the crystal contains regions with saturated FM ordering, since their spontaneous magnetisation does not change in higher fields. This interpretation is additionally confirmed by the fact that a similar rise in magnetisation in weak fields has been observed also in such $LaMnO_3$ specimens whose neutronographic spectra represent superposition of the FM and AFM peaks, and hence which certainly contain the FM phase [78] (Section 4.3).

The magnitude of the total spontaneous magnetic moment is evaluated from the start of the knee on the M vs H curve or by extrapolating the high-field magnetisation to $H = 0$. The magnetic behaviour of doped EuSe is essentially the same.

The presence of FM regions in doped EuTe is confirmed by the Faraday effect data in the range of optical frequencies obtained with the same specimens: doping of EuTe produces a very large Faraday rotation independent of the frequency of the light, which is typical of ferromagnets [15, 19] (Fig. 5). Faraday rotation becomes very small at temperatures above 40 K (Fig. 6). The rise in magnetisation on the M vs. H curve disappears simultaneously.

The possibility that a EuTe crystal, although possessing a spontaneous magnetisation, resides in a uniform magnetic state is ruled out on account of the fact that the Faraday rotation magnitude in the range of fields where the

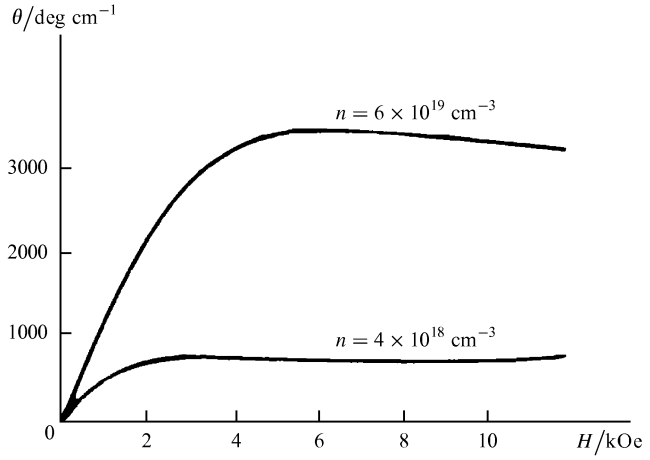

Figure 5. Frequency-independent Faraday rotation θ as a function of the magnetic field H at 8 K for the same EuTe specimens as in Fig. 4 (there is no rotation in the undoped specimen) [15, 19].

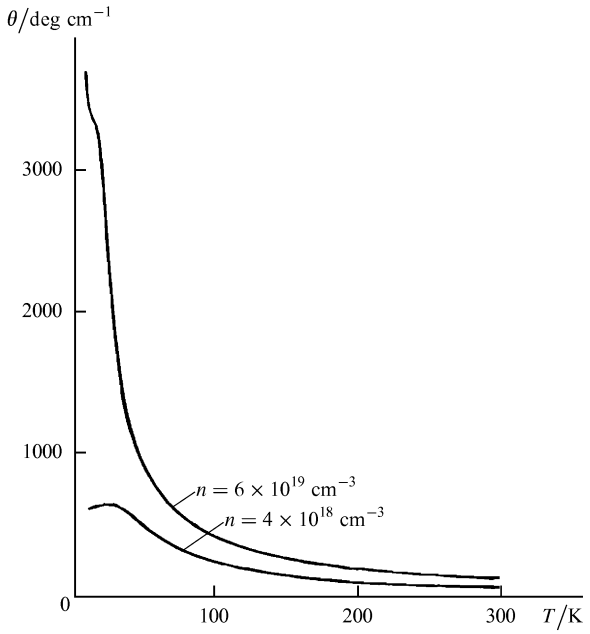

Figure 6. Frequency-independent Faraday rotation θ vs. temperature T in a 10 kOe field for the same specimens as in Figs 4, 5 [19].

magnetisation is a linear function of the field depends very little on the field. In a uniformly-magnetised specimen the rotation would have been proportional to its magnetisation.

Another piece of evidence in favour of the magnetic heterogeneity of doped EuTe crystals is the depolarisation of polarised light propagating in the direction of the 3 kOe magnetic field applied to the specimen [19]. When the beam is at right angles to the field, there is no depolarisation but with such an arrangement there is no Faraday effect either. For this reason the depolarisation of light can be naturally explained as a result of the Faraday magnetic rotation produced by magnetised sections of the crystal, which do not constitute an ideally-periodic structure, and whose dimensions fluctuate. The deviation from the periodicity must be a consequence of the random potential of the impurity atoms. The theory of this effect is developed in Ref. [69] but, unfortunately, lack of some experimental data does not allow its use for establishing the magnetic structure unequivocally.

3.5 Experimental data (electric phenomena)

Results of electric measurements demonstrate that the FM–AFM state can be both insulating and conducting depending on whether the AFM or FM portions of the crystal dominate. In the former case the crystal can be made conducting by destroying its two-phase structure with the aid of a magnetic field or by raising its temperature. This is seen especially clearly in the example of EuSe where the role of donor impurity is played by anion vacancies [18].

Consider two specimens 'b' and 'a' (Fig. 7) whose carrier densities at $T = 300$ K are 7.8×10^{18} and 3.5×10^{19} cm^{-3}, respectively. At relatively high temperatures they behave like typical degenerate semiconductors: the difference in their conductivities is only an order of magnitude at 70 K. However, at 1.6 K the conductivity of the former is almost equal to its high-temperature value, whereas that of the latter is 9 orders of magnitude lower.

A noteworthy point is that the transition of the specimen 'a' to the insulating state takes place simultaneously with the appearance of a spontaneous magnetisation in it, as shown by the magnetisation measurements yielding an M vs. H curve similar to that represented in Fig. 4. This means that the appearance of the FM portion of the crystal is the origin of the insulating state.

But the 10 kOe magnetic field, that induces the transition of the AFM EuSe to the FM state, at 1.6 K reduces the resistance of the specimen 'a' by an enormous amount — by 9 orders of magnitude, whereas the resistance of the high-conductivity specimen 'b' changes little in this magnetic field. The resistivity of this specimen turns out to be much more sensitive to the field in the vicinity of the Curie point (~ 20 K), where the resistivity peak typical of FM semiconductors [9] is situated. This is additional proof that all electrons are concentrated in the FM portion of the crystal.

According to the magnetisation measurements, the FM phase occupies over 60% of the total volume of the crystal in specimen 'b'. It is impossible to evaluate the volume reliably for specimen 'a', but one can be assured that it is small. Hence, one may state that the FM portion of the crystal is simply-connected in specimen 'b' (Fig. 1b) and multiply-connected in specimen 'a' (Fig. 1a). In the former case the conduction electrons, which are concentrated in the FM portion of the crystal, are able to propagate freely in it, and because of that the conductivity of specimen 'b' is high. In the latter case, at $T = 0$, they are confined to separated droplets in specimen 'a', and because of that are able to participate in charge transport only after those droplets have been destroyed by a magnetic field or by rising temperature.

A two-phase conducting state has not been observed in EuTe. The temperature and field dependence of the resistance of a specimen in a two-phase insulating state is qualitatively the same as that for EuSe specimen 'a' [16, 17].

A special discussion is required for the behaviour of phase-separated systems in strong electric fields. One may expect that such fields may cause depinning of charged droplets so that they begin to move throughout the crystal.

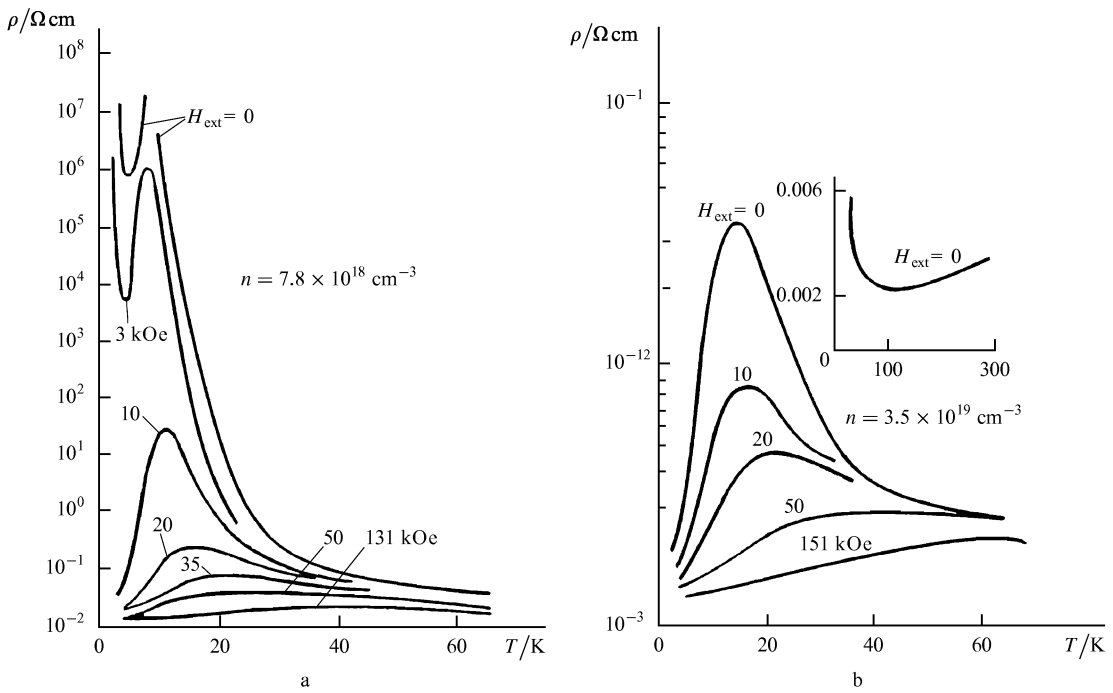

Figure 7. Resistivity ρ in different fields H_{ext} vs. temperature T for EuSe specimens with carrier concentrations n at 297 K presented in Ref. [18].

As the droplets are connected by Coulomb forces their motion should be strongly correlated. Possibly, this effect was observed recently in degenerate EuTe separated in the AFM and FM phases [70, 71]. A rectangular voltage pulse of 10 μs was applied to a sample at 4.2 K. If the voltage is not very high, the response to this pulse repeats its shape. But, beginning from a threshold field of the order of 1 kV cm^{-1}, a sharp peak appears at the trailing edge of the pulse of the current. Its height exceeds the background by several times ten. If the field strength is increased, the peak of the current shifts forwards, and a new peak appears on the trailing edge, and so on (Fig. 8).

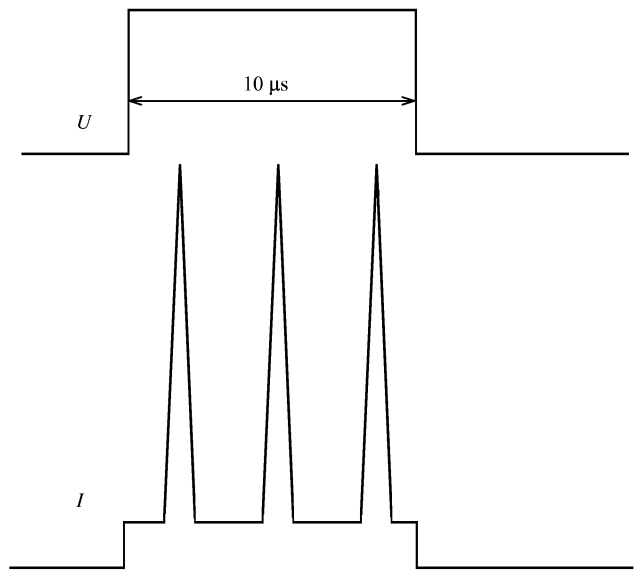

Figure 8. Current I (in arbitrary units) vs. time in doped EuTe as response to a rectangular pulse of voltage U [70].

It is natural to ascribe the rectangular pulse of the current to the conduction electrons thermally excited from the FM droplets into the conduction band of the AFM portion of the crystal. Then the peaks of the current should correspond to the correlated motion of depinned droplets. The electric field tends to orient layers of droplets (Fig. 1a) normally to its direction. Thus, taking into account the correlated motion of droplets, the droplets belonging to the same layer should reach the anode simultaneously. At that moment a peak of the current appears. Then it disappears, and appears again, when the next layer reaches the anode.

One should note that another effect is possible in phase-separated semiconductors: pulsations of the current with charged droplets remaining pinned. Such pulsations do not correspond to a sequence of the peaks of the current as in the case just discussed. On the contrary, they should manifest themselves as vanishing current at certain moments. They should appear due to the N-shaped current–voltage characteristics typical of semiconductors with multiply-charged impurity centres [72]. Here their part is played by the electron droplets. If an electron is thermally excited to the conduction band from such a droplet, then, to return to this droplet, it should surmount the Coulomb barrier created by other electrons remaining inside the droplet. If electrons are heated by a strong electric field they may surmount such a barrier more readily than cold electrons. This diminishes the number of electrons in the conduction band.

Results similar to those described above have also been obtained for Gd_2S_3 with an excess of Gd, where not only the insulating, but also the conducting FM–AFM state has been observed [73, 74]. Possibly the AFM–FM state exists in $GdN_{0.96}O_{0.04}$. The Neel point of this degenerate semiconductor coincides with that of pure GdN but the semiconductor also displays a spontaneous magnetisation [75]. In Ref. [40] the idea was advanced that the two-phase FM–spin glass state is possible. This

assumption may explain the properties of alloys of $xCuCr_2S_4-(1-x)Ga_{2/3}Cr_2S_4$ investigated there.

4. Impurity (chemical) phase separation

4.1 Impurity phase separation in nonmagnetic semiconductors

In this section the phase separation caused by electroactive impurity diffusion will be discussed. The pioneering papers [23, 24], in which impurity phase separation was discovered in degenerate semiconductors with stable phase state, were devoted to the study of Si doped with Li where the atoms remain mobile down to 150 K.

In Ref. [23] the kinetics of Li precipitation at the maximum doping level were investigated. First, indirect proof of the inhomogeneous state was obtained from the time dependences of the conduction electron density n and the Hall mobility in the course of annealing at 300 K and 350 K, which were found to differ strongly from the ordinary kinetics of solid solution precipitation. The assumption was made in Ref. [23] that Li ions which remain electrically active form high density clusters surrounded by depletion regions.

But direct confirmation of the inhomogeneity of Si:Li samples fabricated in the same way as in Ref. [23] was obtained in Ref. [24] during an investigation of plasma infrared reflection $R(\lambda)$. As is well known, this quantity passes a minimum at the plasma frequency which makes it possible to determine the charge carrier density. An additional minimum of $R(\lambda)$ appears at a Hall density n_H exceeding 1.3×10^{19} cm^{-3}. This minimum corresponds to the density $n_0=2\times10^{20}$ cm^{-3} which does not depend on n_H in the region where $n_H\sim10^{19}$ cm^{-3}.

The small amplitude of the signal from the corresponding electron-rich phase shows that this phase is finely divided. The mobility inside electron-rich droplets is four times higher than in the space between droplets which points to some degree of ordering of Li ions inside the droplets.

A similar phenomenon — the existence of two plasma reflection minima — was observed in GeTe enriched with Te (50.1 – 50.8 at.% Te) and annealed at 360 K. The situation here is more complicated than in Si since this material is ferroelectric, and GeTe samples display a domain structure. If the Te content is increased, both the minima λ_1 and λ_2 shift toward the short-wavelength side with simultaneous decrease in the depth of the λ_2 minimum. The depth of the main minimum at λ_1 changed insignificantly in all the samples investigated [25, 26].

The heterophase state is finely divided, and the size of inhomogeneities is, at most, less than 50 μm. They are not related to the fine domain structure. The regions depleted of carriers are likely to be thin layers parallel to the (100) planes.

According to Ref. [26], the resistivity ρ of GeTe as a function of temperature exhibits two peaks between 650 and 750 K. If the total hole density is increased, both the hole densities of the hole enriched and depleted regions increase, but the volume of the latter region is reduced.

Certainly, an explanation of the properties of the degenerate semiconductors just described should be based on the fact that the donor impurity atoms are analogues of the alkaline atoms. The former, like the latter, tend to form a metal consisting of impurity atoms. The role of the crystal is that, firstly, it fixes the volume inside which the impurity atoms are distributed. Secondly, it greatly enhances the impurity atom radius since the true electron mass is replaced by the effective mass, and the energy of the Coulomb interaction is divided by the dielectric constant. This fact was already recognised in Ref. [23].

In Ref. [27] a more rigorous theory of impurity metal was developed. It is based on the following physical picture. The ground-state energy of the impurity metal will have its minimum at a certain density n_{min}. If the Li impurity atoms had been mobile at zero temperature, then, after their introduction into the crystal uniformly at a density less than n_{min}, the system would have become inhomogeneous with all of the Li in a condensate of density n_{min}. For a range of temperatures above absolute zero, the condensate can coexist with a low-density 'vapour' phase. Above a critical temperature only one phase exists, and the system becomes homogeneous.

One may sketch the main ideas of the rather complicated calculation [27] using the simplified jellium model which does not pretend to yield accurate quantitative results. One should consider the total number N of the impurity atoms as fixed and search for the volume V of the impurity metal at which its energy is a minimum

$$E=k\frac{N^{5/3}}{V^{2/3}}-a\frac{N^{4/3}}{V^{1/3}}-bN^{4/3}(cV^{1/3}+N^{1/3})^{-1}\,, \qquad (17)$$

with

$$k=3\frac{(3\pi^2)^{2/3}}{10m}\,,\quad a=3\left(\frac{3}{\pi}\right)^{1/3}\frac{e^2}{4\varepsilon}\,,$$

$$b=0.05647\frac{e^2}{\varepsilon a_B}\,,\quad c=\frac{0.1216}{a_B}\,,\quad a_B=\frac{\varepsilon}{me^2}\,,$$

where m is the effective mass, ε the dielectric constant.

The first term in Eqn (17) corresponds to the kinetic energy of the conduction electrons, the second term to the exchange between electrons with parallel spins, and the third term to the correlation energy between electrons with antiparallel spins [67]. In the last part of this section a refined model of the impurity metal is discussed.

Differentiation of E with respect to V yields the optimum impurity density n_{min} and the energy of the impurity metal per atom $\lambda=E/N$:

$$n_{min}^{1/3}=0.145\,,\quad \lambda(n_{min})=0.0774 \qquad (18)$$

(in atomic units). Thus, the optimum volume V for impurity atoms is equal to N/n_{min}. If it is less than the total volume of the crystal V_t then the crystal should separate into doped and undoped phases.

These phases are electrically neutral, so there are no Coulomb forces leading to their intermixing. Nevertheless, in the equilibrium state the system should consist of alternating layers of different impurity densities: such a geometry reduces the elastic forces caused by the difference in elastic moduli of both phases [28, 29]. Nevertheless, in the case of Si:Li and in many other cases such density domains were not observed.

In my opinion, as the elastic properties of two phases in semiconductors differ only slightly, it is not obvious that they can determine the geometry of the two-phase state. It may be thermodynamically nonequilibrium, determined by the kinetics of phase growth. Formation of single-phase regions may be determined by the distribution of nuclei, and numerous regions of the phase are then analogues of

crystallites in a polycrystal. In any case, both the equilibrium and nonequilibrium sizes of a single-phase region at the impurity phase separation must greatly exceed the size at the electronic phase separation.

The situation in GeTe is more complicated since this crystal is ferroelectric. In such crystals with point defects it is possible to have states with nonuniform density and polarisation distributions. Thus, the polarisation, similarly to the magnetisation, may substantially influence the state of the impurity metal in such a crystal.

4.2 Impurity phase separation in magnetic systems

The impurity phase separation will possess specific features in magnetic crystals only if it can exist at temperatures well below the magnetic disordering temperature. Such a situation is, certainly, possible in magnetic semiconductors with high disordering temperatures. These include many HTSCs and related compounds. In them the two-dimensional AFM correlations may be observed at temperatures above 1000 K. Meanwhile, the excess oxygen atoms which play the part of acceptor atoms may remain mobile down to 200 K [76]. The experimental data available (Sections 5.1, 5.2) shows that, apparently, in most cases phase separation in such materials corresponds to a nonuniform impurity distribution.

In principle, impurity phase separation may exist in magnetic semiconductors of other types. The appearance of two different magnetic phases correlated to different impurity densities is favoured if the difference between the energies of these two phases is small. This does not necessarily mean a low temperature of magnetic disordering: it is sufficient that in the space of the exchange integrals the system considered is not very far from the boundary between these two phases (see Section 2.4).

On the other hand, the impurity–magnetic phase separation is possible even in materials with low temperature ordering if the phase, appearing as a result of local increase in the impurity density, has a high ordering temperature. Finally, the nonuniform impurity distribution, established at elevated temperatures where the atom mobility is high but the magnetic ordering is destroyed, may remain in thermodynamic equilibrium at low temperatures where the impurity is frozen but magnetic ordering exists. If this is not the case and the impurity distribution at low temperatures is not in equilibrium, the electron phase separation may occur on the basis of the nonuniform impurity distribution.

In what follows, the magnetic–impurity phase separation will be considered in an AFM heavily doped semiconductor with allowance for the fact that the mobile electrons tend to establish the FM ordering (Section 2.3). To solve this problem, it is necessary to determine the energy as a function of the magnetisation. One should take into account the following very important circumstance: the indirect exchange via conduction electrons in degenerate magnetic semiconductors is essentially non-Heisenbergian.

In fact, the Heisenberg indirect exchange Hamiltonian is obtained from the Hamiltonian of the $s-d$ model (1) in the second order in the small parameter AS/μ. But even in the case $AS/W \ll 1$ considered here the parameter AS/μ according to Eqn (2) is large for degenerate semiconductors, which excludes the possibility of standard treatment of the indirect exchange. As shown in Ref. [9], this non-Heisenbergian indirect exchange in degenerate semiconductors leads to the appearance of a range of electron densities inside which both AFM and FM orderings are unstable in the isotropic three-dimensional case.

In this range the canted AFM ordering is energetically more favoured than the AFM or FM orderings. In addition, the canting angle changes continuously with the electron density, allowing a continuous transition from AFM to FM structure. But one may prove that the minimum for the energy of the system is absent from this range [30].

The main difference between nonmagnetic and magnetic phase separation is that even at $T = 0$ the energy of the magnetic impurity metal is a minimum not at one but at two densities (when considering the $T \ll T_N$ region, one may put $T = 0$). In what follows, we will consider the energy minima at the AFM and FM orderings without a detailed analysis of the maximum between them, omitting the cases when the minimum energies are attained at the stability boundaries of the collinear phases (these cases are treated in Ref. [30]). Then in the zeroth approximation in AS/W the optimum density in the AFM phase ν_A is determined by the condition of minimum energy (17). The reason for this is the following: at the AFM ordering the $s-d$ shift of the total electron energy is proportional to A^2S^2N/W and, hence, does not depend on the volume V of the impurity metal.

Now we investigate the possibility of establishing FM ordering in a doped AFM crystal. In treating this problem, one should take into account the energy expenditure $D = |J|S^2$ for replacing the AFM ordering by the FM ordering. Then the equilibrium impurity density should be determined from the condition of minimum energy

$$E_{FA} = E_F + D\frac{V}{v} - AS\frac{N}{2} \tag{19}$$

($v = a^{-3}$). The electron–impurity energy E_F should be written with allowance for the fact that according to Eqn (2) the conduction electrons are completely spin-polarised. For this reason their kinetic energy is higher, the exchange interaction stronger, but the correlation energy is absent from the total energy E_F:

$$E_F = 2^{2/3}k\frac{N^{5/3}}{V^{2/3}} - 2^{1/3}a\frac{N^{4/3}}{V^{1/3}}. \tag{20}$$

Minimisation of Eqns (19), (20) with respect to V under the assumption that D exceeds the energy of exchange between electrons leads to the following expressions for the optimum impurity density ν_{FA} and the impurity metal energy per atom λ_{FA}:

$$\nu_{FA} = \nu_{FA}^0 + \nu_{FA}^1; \tag{21}$$

$$\nu_{FA}^0 = \frac{1}{2}\left(\frac{3D}{kv}\right)^{3/5}, \quad \nu_{FA}^1 = \frac{3a}{20k}(2\nu_{FA}^0)^{2/3};$$

$$\lambda_{FA}(\nu_{FA}) = (2D)^{2/5}\mu^{3/5}(\nu^{-1}) - \frac{AS}{2}, \tag{22}$$

$$\mu = \frac{(3\pi^2 n)^{2/3}}{2m}.$$

As mentioned above, the possibility of the impurity–magnetic phase separation is a consequence of the existence of two energy minima: one at the AFM ordering and the other at the FM ordering (Fig. 9). According to Eqns (18)

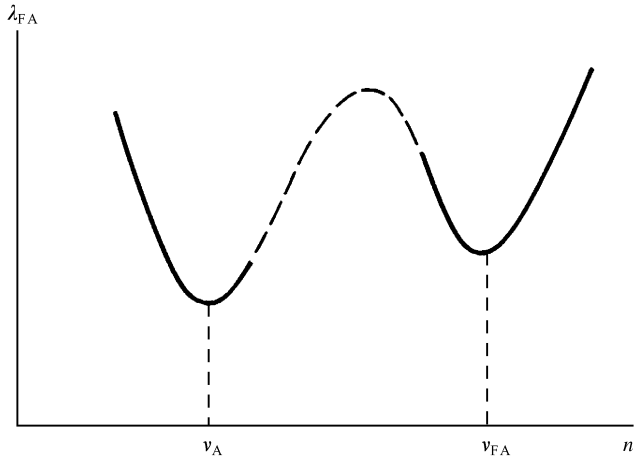

Figure 9. Energy of impurity metal per atom in an antiferromagnetic crystal tending to become ferromagnetic vs. the average impurity atom concentration. Solid lines correspond to AFM and FM structures, the dashed line to the intermediate canted state.

and (19), at large enough D the former corresponds to a lower density than the latter.

Let us first discuss the case when the deepest energy minimum corresponds to the FM ordering (at v_{FA}). If the density n is less than v_{FA} all the impurity atoms are concentrated in the region with the FM ordering occupying the n/v_{FA}-th portion of the crystal. The rest of the crystal is AFM and insulating owing to the absence of the donor impurity from it. In this respect the situation resembles the situation at the electronic phase separation, though the mutual charging of phases and, hence, intermixing of phases on the nanometer scale is nonexistent here.

Let us assume now that the energy minimum for AFM ordering is deeper than for FM ordering. The case will be considered when the mean density n exceeds the density v_A, at which the minimum is reached. If n lies between the energy minimum and the stability boundary of the AFM phase, then it will be assumed that the energy of the AFM structure per impurity atom $E_A(n)/N$ exceeds the minimum energy for FM ordering λ_{FA}. No special assumptions are required when n lies inside the instability range for the collinear structures. In both cases separation of the impurity atoms into two phases should occur. In one of them the ordering is AFM, and in the other FM. Their impurity densities ζ_A and ζ_F are determined by

$$\frac{\partial E}{\partial N_A} = \lambda(\zeta_A) - \lambda_{FA}(\zeta_F) + \zeta_A \frac{\partial \lambda_A}{\partial \zeta_A} - \zeta_F \frac{\partial \lambda_{FA}}{\partial \zeta_F} = 0 , \quad (23)$$

$$\frac{\partial E}{\partial V_A} = \zeta_A^2 \frac{\partial \lambda_A}{\partial \zeta_A} - \zeta_F^2 \frac{\partial \lambda_{FA}}{\partial \zeta_F} = 0 , \quad (24)$$

where E is the total energy of the system. Obviously, Eqns (23) and (24) express the equality of chemical potentials and pressures in both phases.

Using quadratic approximations for the energies per atom in the AFM and FM phases, λ_A and λ_{FA}, in the vicinity of v_A and v_{FA}, one may readily obtain explicit expressions for the densities sought, and, hence, for the volumes of these phases V_A, V_F and the numbers of atoms in them N_A, N_F.

A basic difference between the previous case and the case under discussion is that not only the FM but also the AFM phase is highly conductive here. This is a consequence of the fact that the former is not energetically favoured compared with the latter. Thus, it is not energetically favourable for all the impurity atoms to concentrate inside the FM phase but only for part of them. Meanwhile, as the impurity density in the FM phase is higher than in the AFM phase, the conductivity of the former should remain higher than that of the latter.

The initial AFM phase may coexist not only with the FM phase but also with other phases in which the charge carrier energy is lower. In full analogy with the electron phase separation, the impurity phase separation is possible with the formation of a new AFM or spin-liquid phase.

As in Section 3.2, the staggered AFM phase with the structure vector $\boldsymbol{Q} = (\pi, \pi, \pi)$ will be considered as the initial phase and the layered phase with $\boldsymbol{Q}' = (\pi, 0, 0)$ as the phase produced by doping. Unlike the FM ordering, the layered ordering cannot be obtained from the staggered ordering by a continuous transformation. Thus, the curve of the energy dependence on the density for the impurity metal is the superposition of curves corresponding to both types of ordering (Fig. 10). The curve for the staggered ordering $E_A(n)$ is described by Eqn (17), and that for the layered one by

$$E'_A = E_A + D' \frac{V}{v} - [g(\boldsymbol{Q}') - g(\boldsymbol{Q})]N \quad (25)$$

where $D' = (-4I_1 + 8I_2)S^2$, $g(\boldsymbol{Q}) = A^2S^2/4(E_{\boldsymbol{Q}} - E_0)$.

An analysis of Eqn (25) is carried out in close analogy with Eqn (19). Quite similarly, the possibility of coexistence of highly-conductive regions with staggered and layered orderings may be proved, the former with reduced and the latter with enhanced impurity density.

As discussed in Section 2.4, the s-electron energy in the magnetically disordered spin-liquid phase is close to the energy inside the layered AFM phase, and the energy D_{SL} expended for the spin disordering may be well below the rearrangement energy D' from the staggered to the layered

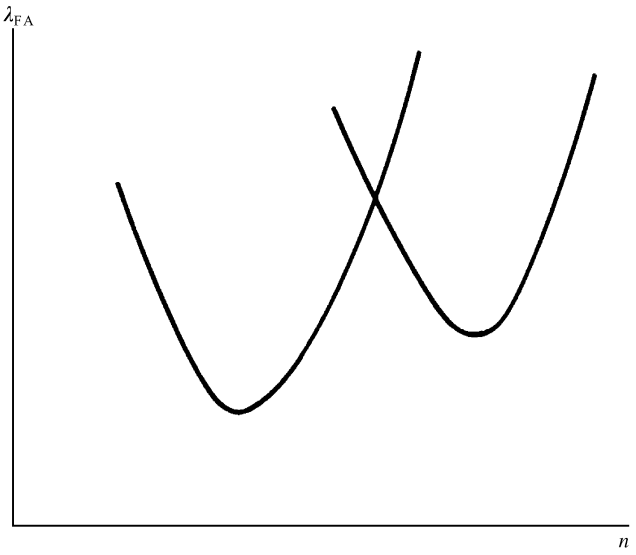

Figure 10. Energy of impurity metal per atom vs carrier density in an antiferromagnetic crystal tending to change its type of antiferromagnetic structure.

phase. Thus, in describing the spin-liquid impurity metal, one should replace D' by D_{SL} in (25) and $g(\boldsymbol{Q}')$ by

$$g_{SL} = -A^2 S^2 (2\pi)^{-3} \nu \int d\boldsymbol{k}\, (E_k - E_0)^{-1} . \qquad (26)$$

In the nearest neighbour approximation for E_k the quantities g_{SL} and $g(\boldsymbol{Q}')$ are practically equal for the isotropic three-dimensional case.

As was discussed above, in the case of the single-electron phase separation, one cannot make the unambiguous conclusion that the spin-liquid state can coexist with the staggered AFM phase: possibly, the FM state in such cases is still more energetically favoured. In the case of impurity phase separation, conditions for the formation of a spin liquid instead of an FM region are still more favourable compared with the single-electron self-trapping. In fact, the energy of the impurity metal in the FM region is increased as compared with the spin liquid due to the electron spin polarisation [c.f. Eqns (17) and (20)]. Thus, the antiferromagnetic – spin-liquid phase separation accompanied by the impurity density separation may be preferable under certain conditions.

4.3 Large-scale phase separation in $LaMnO_3$

In the next section examples will be given of HTSCs with firmly established phase separation. But here a specific material with very interesting physical properties — $LaMnO_3$ — will be described though there is no direct evidence yet that the phase separation in it is just the impurity phase separation. However, I do not see any other way of explaining its properties.

Undoped $LaMnO_3$ has a layered AFM structure with a very small moment canting of relativistic origin [77]. Under normal conditions only Mn^{3+} ions are present. However, doping with Ca, Sr or heat treatment in an oxygen atmosphere produces Mn^{4+} ions, as a result of which the crystal acquires much larger spontaneous magnetisation [78–81] (Fig. 11).

For small concentrations $n(Mn^{4+})$ the magnetisation grows with n and attains the maximum corresponding to perfect FM order at $n \sim 30$ at.%, after which it starts falling again. In the range of smaller concentrations of Mn^{4+} the neutron spectra at 4.2 K represent a superposition of spectra corresponding to AFM and FM ordering [78]. Fig. 12 depicts the spectrum of a specimen with 18 at.% Mn^{4+}. AFM peaks are shaded, other peaks are FM.

In principle, such spectra may be associated both with the two-phase FM – AFM state of a specimen and with the single-phase two-sublattice one with a nonzero moment (canted or ferrimagnetic). A unique choice between the two is made possible by studying the spectra as functions of the magnetic field [78]. When the field is directed along the neutron scattering vector $\boldsymbol{q}$, FM peaks must become lower (vanishing altogether in the high-field limit), since the intensity of the FM scattering is proportional to $(1 - |\boldsymbol{q}\cdot\boldsymbol{m}|^2)$, where $\boldsymbol{m}$ is the unit vector pointing in the direction of the moment [82].

On the other hand, the intensity of AFM scattering is proportional to $(1 - |\boldsymbol{q}\cdot\boldsymbol{l}|^2)$, where $\boldsymbol{l}$ is the AFM unit vector. In the case of a two-phase system with the $\boldsymbol{m}$ and $\boldsymbol{l}$ vectors not interconnected, a weak magnetic field will rotate only the magnetism vector $\boldsymbol{m}$, not affecting the AFM vector $\boldsymbol{l}$, i.e., AFM scattering will remain unchanged. On the other hand, in the case of a single-phase system, the vector $\boldsymbol{l}$ will rotate together with the vector $\boldsymbol{m}$. Hence, both FM and AFM scatterings will change simultaneously.

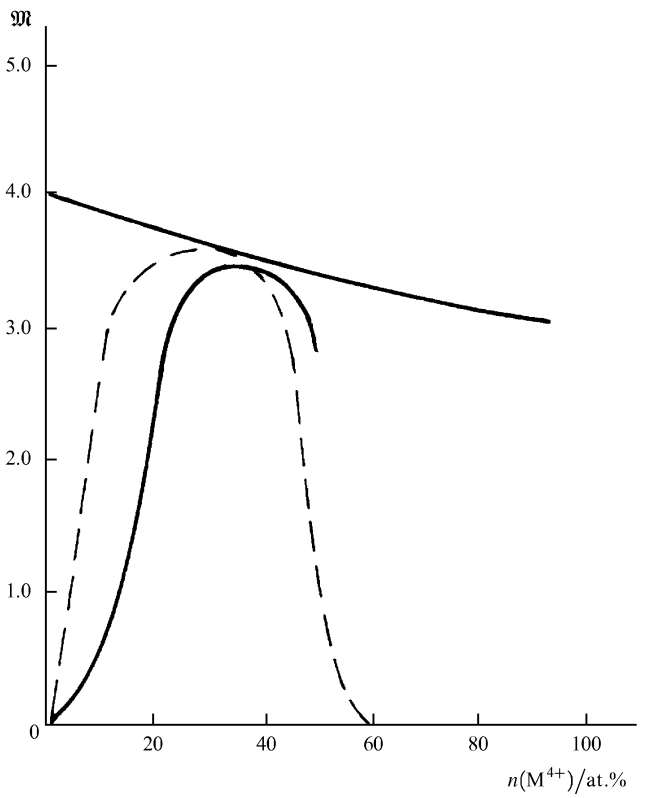

Figure 11. Magnetisation vs. concentration of Mn^{4+} ions for $La_{1-x}Ca_xMnO_3$. Solid line from Ref. [78], dashed line from Ref. [79].

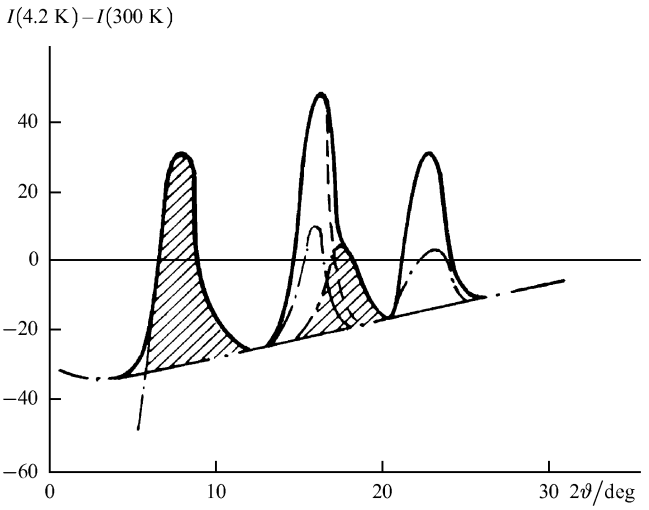

Figure 12. Neutron scattering intensity vs. scattering angle 2ϑ in $La_{1-x}Ca_xMnO_3$ with 18 at.% Mn^{4+} at 4.2 K minus the intensity at 300 K (in arbitrary units). Shaded peaks are antiferromagnetic, unshaded ferromagnetic. Dashed lines depict the same spectrum in a 4.5 kOe field [78].

Fig. 12 shows clearly that a field of 4.5 kOe reduces FM scattering by more than a half and has no effect whatsoever on the AFM scattering. Hence, one may conclude that the crystal is in a two-phase AFM – FM state.

Research on the electric properties of doped $LaMnO_3$ [79–83] demonstrates that crystals displaying pure FM

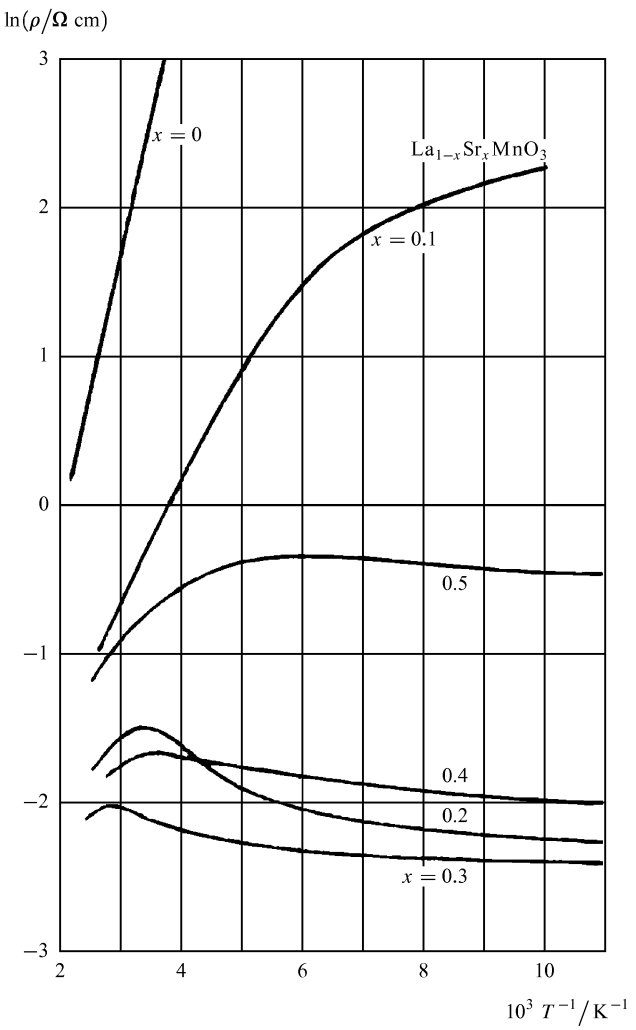

Figure 13. Resistivity vs. temperature for $La_{1-x}Sr_xMnO_3$ [79, 83].

ordering (30–40 at.% Mn^{4+}) also have a high metallic conductivity. The conductivity of two-phase specimens with a small relative volume of the FM portion ($\sim$ 10 at.% Sr, i.e., the same amount of Mn^{4+}) is very small at low temperatures, growing exponentially with the temperature. But the main portion of a two-phase specimen with 20 at.% Mn^{4+} is FM. This sample possesses a high conductivity (Fig. 13).

Thus, one sees that conducting portions are FM and nonconducting portions are AFM as in EuSe (Section 3.4). But the fact that both the FM and AFM peaks in Fig. 12 are well defined suggests that the FM and AFM regions are quite large. In the case of the electronic phase separation the minority phase regions are very small because of the Coulomb forces (Section 3.2). Thus, one may expect that the electronic phase separation does not occur here: droplets would manifest themselves only in small-angle neutron scattering.

Phase separation in $LaMnO_3$ is also confirmed in Ref. [84] where it is explained by the appearance of different crystallographic phases in this material.

5. Phase separation in high-temperature superconductors

5.1 Phase separation in La_2CuO_4-based materials

The first indirect indications that phase separation is possible in HTSCs were obtained almost simultaneously with their discovery in pioneering investigations [85, 86] of La_2CuO_4-based materials.

Though phase separation in stoichiometric La_2CuO_4 was not found, soon direct experimental proof of the phase separation in $La_2CuO_{4+\delta}$ was given. First, neutronographic studies should be mentioned. According to Refs [87, 88], below 320 K this crystal becomes reversibly separated into two different phases with crystallographic structure very similar to each other. One of them has stoichiometry near La_2CuO_4. The second phase is an oxygen-rich phase that is superconducting with transition temperature $T_c = 38$ K. The abundance of the second phase increases with the oxygen pressure at which the samples are annealed. One may evaluate the size of single-phase regions from the width of the neutron scattering peak: it is about 300 nm. Similar investigations [76] show that values of δ in the two coexisting phases are about 0.01 and 0.06, and the difference in δ disappears abruptly at 265 K, on increase in temperature. The phase separation in $La_2CuO_{4+\delta}$ is also confirmed by neutron spectroscopy investigations in Ref. [89].

Another direct confirmation of phase separation in this material was given by NMR hyperfine field measurements [90, 91]. They made it possible to establish that a portion of the Cu ions is nonmagnetic whereas the rest is magnetic in the Mott-insulating d^9-Cu^{2+} state of the stoichiometric La_2CuO_4 [90].

In Ref. [91] two signals were observed, one originating from regions of the crystal rich in oxygen and a second having no excess oxygen. Upon warming through 265 K the volume fraction of the crystal poor in oxygen goes to zero. The magnetic shift of the peak intensity of the line originating from the oxygen-rich portion of the crystal does not change in the vicinity of 265 K.

These results agree with results obtained by other methods. In the first paper [92] superoxygenated $La_2CuO_{4+\delta}$ was investigated by the following means: resistivity, Seebeck and Hall coefficients, magnetoresistance, electron microscopy, ac and dc susceptibility, and specific heat. Below 300 K the material has a fine-grained microstructure which is a mix of nonmagnetic $La_2CuO_{4.05}$ and insulating AFM La_2CuO_4. In the second paper [92] magnetic and electric measurements reveal anomalies between 200 and 280 K that are attributed to a phase separation involving oxygen diffusion.

An extensive study of the system under discussion was carried out in Ref. [93] where the phase separation in $La_{2-x}Sr_xCuO_{4+\delta}$ was investigated as a function of two parameters x and δ simultaneously in their range from 0 to 0.03. The fact of the phase separation was established from the curve describing dependence of susceptibility on T. If this curve displays a peak it is associated with the insulating AFM phase. But if, on decrease in temperature, a sharp drop in susceptibility begins about 35 K, such a 'knee' in the curve is interpreted as a signature of the transition to the superconducting state (Fig. 14).

In absence of excess oxygen, phase separation at low Sr doping was not observed. In my opinion, this is a result of

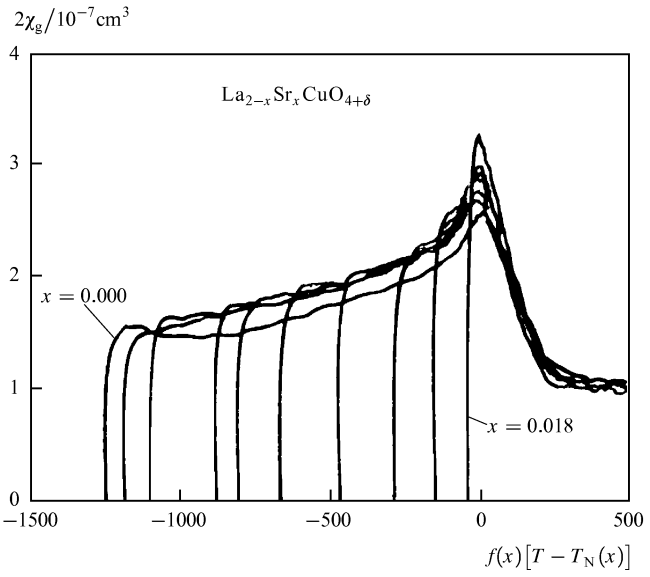

Figure 14. Temperature dependence of the magnetic susceptibility χ_g of $La_{2-x}Sr_xCuO_{4+\delta}$ samples annealed in 1 bar O_2 presented in terms of a scaling function $f(x)$ determined experimentally, and the Neel temperature $T_N(x)$ [93].

low Sr atom diffusion. On increase in x, the Neel temperature decreases rapidly from 300 K at $x = 0$ to 0 K at $x = 0.02$. At x exceeding 0.02, the spin-glass state is observed below 10 K, and the superconductivity appears only at x values between 0.1 and 0.25.

In samples with excess oxygen ($\delta \cong 0.03$), introducing Sr suppresses the phase separation which disappears at $x = 0.03$. In phase-separated samples the Neel temperature in the AFM nonsuperconducting phase decreases with increasing x, following the finite-size scaling law. From this fact the conclusion can be drawn that the finite-size effects are caused by doping. This results in a new separation of holes introduced into samples: they concentrate in walls between macroscopic regions of the undoped material. However, it would be desirable to obtain direct experimental confirmation of such a complicated picture of the phase separation.

The above conclusion about the absence of any magnetic ordering in the superconducting phase is not quite accurate. Muon spin rotation experiments performed on superconducting $La_{2-x}Sr_xCuO_4$ [94] show that internal magnetic fields coexist below 2 K with superconductivity for $x \leqslant 0.15$. The magnetic fields in the superconducting state are an order of magnitude smaller than the corresponding fields in undoped La_2CuO_4. These results suggest that magnetic correlations exist in the investigated material even in the superconducting state.

One should also keep in mind that the magnetic structure of the stoichiometric AFM La_2CuO_4 is rather complicated: a small magnetic moment canting of relativistic origin was observed. But this canting has opposite direction in neighbouring magnetic planes so that the total moment of the crystal is zero. A relatively small magnetic field makes the direction of canting the same for all the magnetic planes [95].

One might believe that the difference in the parameter δ for two phases is itself sufficient to justify the statement that the phase separation in $La_2CuO_{4+\delta}$ is of impurity (i.e., of chemical) nature. Such an interpretation agrees with the large size of single-domain regions found in Ref. [87]: this is possible only if the regions are electroneutral. However, this point of view on the phase separation in $La_2CuO_{4+\delta}$ is not supported in Refs [96, 97].

In the first study [96] it was established that the phase separation could be suppressed by a rapid cooling and restored by a magnetic field of 3 T. These results are interpreted in terms of the appearance of magnetically-polarised quasiparticles (analogues of ferrons, Section 2.3) which unite, forming a percolative conducting, and below 37 K a superconducting phase (cf. percolation of the electron liquid in Sections 3.1–3.3).

In the second study [97] the mechanisms driving the phase separation in this material were studied by magnetic susceptibility and electrical resistivity measurements on specimens subjected to different thermal treatments. The phase separation has started to develop by 150 K and becomes rather pronounced above 180 K as is shown by an increase in diamagnetic response. Meanwhile, the oxygen diffusion becomes substantial only at 230–250 K. It leads to the destruction of the superconducting phase, hence refuting the common opinion that oxygen diffusion supports superconductivity.

An important role which, in the opinion of the authors of Refs [96, 97], low-temperature diffusion of holes plays in the appearance of superconductivity and phase separation supports the idea of electronic phase separation in this material (see also Ref. [98]).

Of the latest studies on this material, Ref. [99] is of fundamental importance. In this study conditions were created such that when $\delta = 0.03$ phase separation does not occur. For this experiment a crystal of very high quality was used, in which the oxygen diffusion was suppressed due to the absence of structured imperfections that facilitate this process. Respectively, such a uniform crystal displays the transition into the superconducting state as a whole, but the temperature of this transition is low — about 12 K. Meanwhile, in a more imperfect crystal with $\delta = 0.04$ the phase separation takes place with the temperature of the superconducting transition close to 40 K. This confirms experimentally that phase separation creates favourable conditions for superconductivity.

The physical reason according to which phase separation facilitates superconductivity is quite obvious. At relatively small acceptor impurity density the temperature of the superconducting transition increases with the hole density. The phase separation just leads to an increase in the impurity density, i.e. in the hole density in one of the phases and, hence, increases this temperature in it.

5.2 Phase separation in other HTSCs

Many other HTSCs are found to exhibit phase separation, among them $YBa_2Cu_3O_{7-\delta}$. In Ref. [100] the magnetisation curves of this material display a pronounced low-field minimum below T_c which correlates with the c-axis lattice parameter and, hence, with δ. This low-field feature is interpreted in terms of a field-induced decoupling of regions of oxygen-rich material by boundaries of oxygen-poor materials. Phase separation in the yttrium ceramic is indicated also by a plateau in the composition dependence of the transition temperature [101].

Direct proof of the phase separation in $YBa_2Cu_3O_x$ ($6.0 < x < 7.0$) was obtained using Mossbauer spectro-

scopy [102]. The amount of the sample which is superconducting depends on x strongly increasing: from zero at $x = 6.50$ to about 50% at $x = 6.56$, to about 75% at $x = 6.66$, and reaching 100% as x approaches 7.0. The remaining fraction of the probes shows a concomitant decrease in importance with increasing x, and continues to exhibit spin glass-like behaviour.

It is very interesting that $YBa_2Cu_3O_{7-\delta}$ is likely to display not only thermal equilibrium but also photoinduced phase separation with the appearance of superconductivity [103 – 105] which may be proof of the electronic mechanism of phase separation in it. The temperature dependences of the transient photoinduced conductivity at different light intensities and of the doping-induced conductivity at different δ are similar, indicative of 'photodoping'.

For $\delta = 0.7$, signatures of the photoinduced transition to metallic behaviour are observed at large enough intensities. The deep resistivity minimum below 100 K reminiscent of the onset of superconductivity in granular superconductors and in inhomogeneously doped samples (see Ref. [106]) was interpreted in terms of phase separation and metallic droplet formation. For $\delta = 0.6$, the lifetime of the photoexcited state is enhanced by nearly 3 orders of magnitude at high excitation levels, indicative of metastability. (The theory of photoinduced phase transitions in magnetic semiconductors is presented in Refs [107, 108]).

Very interesting results concerning phase separation in HTSCs were obtained in Ref. [109] where neutron scattering was used for investigation of crystalline fields in $ErBa_2Cu_3O_x$. Three cluster types were discovered in this material. Two of them correspond to metallic regions with superconducting transition temperatures of 90 K and 60 K, respectively. The third type corresponds to semiconducting regions.

Fig. 15 shows the fractional proportions of the three cluster types and exhibits a continuous behaviour versus the oxygen content, confirming that the transfer of holes into the CuO_2 planes is linearly related to the oxygenation process. These proportions may be explained as follows. For $x = 6$ the system is a perfect semiconductor. In it the oxygen may occupy sites not only in Cu–O planes but also in Cu–O chains. When oxygen ions we added into the chains, holes are continuously transferred into the CuO_2 planes. By this mechanism the number of local regions with metallic character rises. These can partially combine to form larger regions. For some critical concentration a percolative network is built up, and the system undergoes a transition from the semiconducting to the conducting state with a superconducting transition temperature T_c of 60 K.

Upon further increase in the hole concentration, a second (different) type of metallic cluster is formed. These start to attach to each other and at the percolation limit induce a transition into another conducting state with T_c of 90 K.

In the same material neutron diffraction and ac susceptibility provide evidence of structural inhomogeneities near the tetragonal-to-orthorhombic transition which can best be described as a mixture of the corresponding phases [110].

In a certain sense, fundamental results were obtained in Ref. [111]. Mossbauer effect studies of electron HTSC $Nd_{2-x}Ce_xCuO_4$ show that all the oxygenated and 'deoxygenated' samples with $x = 0.00$, 0.14, 0.16, and 0.18

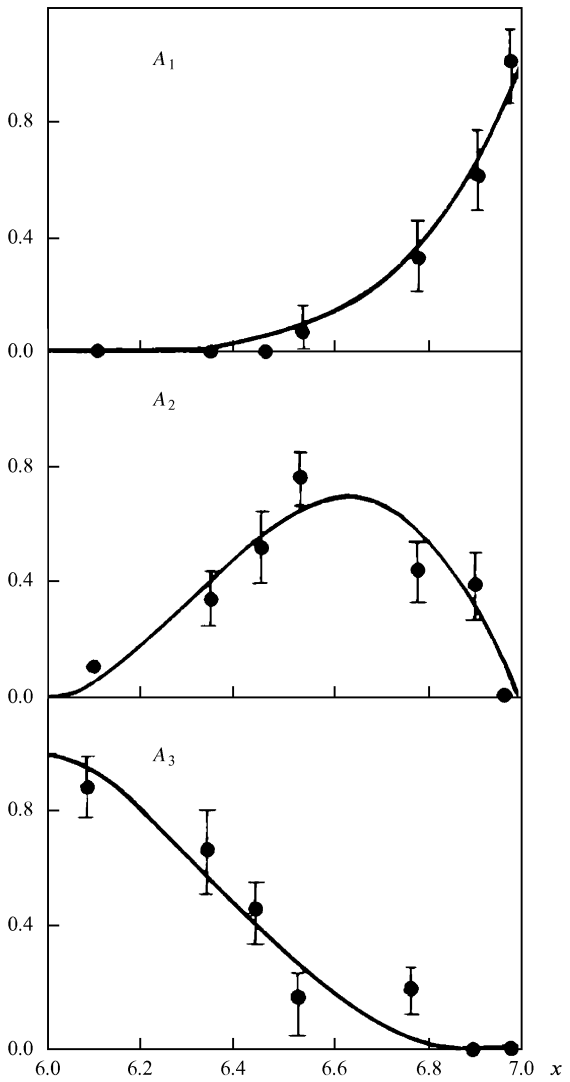

Figure 15. Fractional proportions of the three cluster types in $ErBa_2Cu_3O_x$ as a function of the oxygen content. A_1, A_2, and A_3 corre-spond to metallic clusters with superconducting transition temperatures $T_c = 90$ K, $T_c = 60$ K, and to semiconducting clusters [109].

contain large proportions of microscopic spin clusters. Even in the deoxygenated ceramic with $x = 0.16$, superconducting regions coexist with about 53% of microscopic spin clusters of typical size ~2.5 – 25 nm. Spin cluster formation is induced by extraneous oxygen occupying axial apical positions.

It is confirmed in Ref. [111] that 2-D magnetic order in the electron-doped system is much stronger than that in hole-doped systems, with extremely long-lived spin correlations far above the 3-D Neel temperature.

Another system which exhibits phase separation is $Bi_2CaSr_2Cu_2O_x$. Its XRD pattern is indexed on the basis of the orthorhombic structure. However, three additional peaks which could not be indexed may correspond to a minor second phase present in the sample [112].

Similar results were obtained in Ref. [113] where samples with nominal composition $Bi_{2-x}Pb_xSr_2Ca_2Cu_3O_y$, $0 \leqslant x \leqslant 2$ were investigated. It was established by means of XRD and scanning electron microscopy that Bi – HTSCs with T_c of 80 K and of 110 K

normally coexist. From $x = 0.5$ upwards a nonsuperconducting almost Bi-free second phase appears.

Given that there are examples of phase separation in materials containing magnetic ions, it should be noted in particular that phase separation, apparently, was observed also in HTSCs not containing magnetic ions. The $Ba_{1-x}K_x$-BiO_3 ceramic displays an anomalous nonlinear behaviour of resistivity ρ below $T_c = 30$ K. A 'dielectric' enhancement of ρ is observed at 'large' currents. The value of ρ is several orders of magnitude higher than ρ in the normal phase but it is suppressed by the magnetic field equal to the critical field at 'small' currents through the sample. A nonmonotonic temperature dependence of the critical current and reentrant superconductivity with respect to $\rho(T)$ were observed [114].

In Ref. [114], as well as in Ref. [22], these effects were explained by separation of a sample into alternating superconducting and insulating phases. The former are connected to each other through the insulating phase, and the magnetic field destroys these connections, which leads to a large resistance.

5.3 Theoretical problems of phase separation in HTSCs

First of all, it should be pointed out that by no means is phase separation a necessary condition for superconductivity: many HTSCs do not exhibit this phenomenon. On the other hand, there are nonsuperconducting materials exhibiting phase separation. Thus, one may only hope that in some cases the phase separation creates favourable conditions for superconductivity by ensuring optimum magnetic order and charge carrier density.

One may also expect that superconductivity cannot influence phase separation substantially since the superconducting gap does not exceed 0.01 eV, i.e. is small compared to other typical electronic energies. Moreover, if the phase separation is a result of the impurity atom diffusion, this process turns out to be frozen at temperatures considerably exceeding the transition temperature to the superconducting state. In other words, it occurs in the normal state of the material (e.g., in $La_2CuO_{4+\delta}$ with $T_c = 38$ K the phase separation occurs at about 200 K). Cases where phase separation takes place in the superconducting state are unknown as yet. This shows that the very fact of superconductivity should not be taken into account in a theoretical treatment of phase separation.

If the phase separation does not reduce to nonuniformities in the impurity distribution, then it can occur only if energy expenditures for phase transformation are small. This condition may be met not only in magnetic materials, but also in nonmagnetic materials with a lattice of easily changed state. As was already pointed out in the previous section, apparently, phase separation exists in nonmagnetic HTSCs, too, though this problem requires additional experimental investigations. In particular, it must be proved that it is not a pure impurity phase separation. If so, then in such HTSCs the lattice mechanism of phase separation should occur. Its different versions are developed in Refs [20–22, 115]. But this mechanism is beyond the scope of the present review.

Now we return to magnetic mechanisms of phase separation. One may expect that in cases when an HTSC may be described by the $s-d$ model with a weak $s-d$ coupling, the theory presented in Section 3.2 is applicable to it after its generalisation to the quasi-two-dimensional case (Section 5.4). But one should keep in mind that the two-phase AFM–FM state with charge carriers concentrated in the FM phase [3, 4] can hardly be achieved in superconductors. The singlet pairing in the FM phase is impossible. Though the triplet pairing is theoretically possible nobody has observed the coexistence of superconductivity and ferromagnetism so far.

Experimental results [111] are not at variance with this statement since there is no proof that the FM clusters inside the nonferromagnetic superconducting host are also superconducting. The fact that the host is metallic may indicate the impurity nature of the phase separation in this material (Section 4.2) because at the electronic phase separation all the charge carriers should be concentrated in the FM portion of the crystal (Section 3.2).

But the theory of separation into an insulating AFM and conducting AFM or spin-liquid phase [13, 55] may be immediately valid for HTSCs, too.

An alternative to the $s-d$ model with a weak or intermediate $s-d$ coupling is the Hubbard model with a strong on-site repulsion, and the $t-J$ model closely related to it. The latter is very often used for description of HTSCs though such a possibility is not always self-evident (see Section 2.1). Qualitative results following from these alternative models may differ strongly.

For example, in the $s-d$ model with a weak $s-d$ coupling at small J the single-electron phase separation (the ferron state, Section 2.3) is possible. But in the $t-J$ model at small J it is impossible. In fact, if the model of a classical antiferromagnet with alternating up and down spins is adequate, in the limit of very small exchange, not the ferron but another quasiparticle is the most energetically favoured in the $t-J$ model. In the pioneering study, Ref. [116], it was called the quasioscillator and now is known under the title 'magnetic string'.

Unlike the ferron, the string does not possess a giant magnetic moment and has nothing in common with heterophase self-trapping. It corresponds to simultaneous oscillations of the charge carrier and magnetic disordering. The latter has an antiphase AFM structure which appears along the carrier path when it moves from its equilibrium point [(0, 0) Fig. 16b, c]. It disappears when the electron returns to its equilibrium point along the same path. The equilibrium point moves throughout the crystal due to the zero-point spin oscillations and closed paths [117].

If one uses the Ising model for the 2-D case one finds that the string energy counted off from 'the conduction band bottom' $(-4|t|)$ is of the order of $|I/t|^{1/6}$ times less than the ferron energy. A similar inequality is also obtained for 3-D Ising and Heisenberg models [118]. For the 2-D

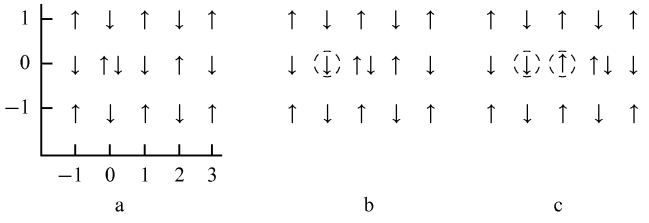

Figure 16. Magnetic string (quasioscillator) in an antiferromagnet with staggered ordering. Motion of the conduction electron begins from the equilibrium point (0,0).

Heisenberg model the corresponding treatment has not been carried out yet, since the 2-D zero-point spin oscillations are very large, and the classical model of an antiferromagnet may be inapplicable here. Nevertheless, a large magnetic anisotropy in CuO_2 planes [95] gives hope for its applicability. The strings are more promising for superconductivity than the ferrons since they do not cause the appearance of ferromagnetism.

Thus, even states of single charge carriers are unknown in the 2-D $t-J$ model. One may only expect that the probability of the charge carrier interatomic transitions increases due to strong zero-point spin oscillations, and, respectively, their tendency to self-trapping reduces still more. Moreover, the many-electron problem is still far from being solved. Nevertheless, numerous attempts to solve the problem of phase separation within the framework of this model have already been made. All of them correspond to the electronic phase separation.

Chronologically, Refs [97] were the earliest in this field. They are based practically on the ferron model, and their authors themselves claim that their model differs from my ferron model only by the smaller size of their quasiparticles (but in Ref. [9] small ferrons are treated, too). On increase in the number of holes, they form a percolation structure leading to the appearance of superconductivity in a sample. Such percolation resembles the percolation predicted in Ref. [4] (Section 3.1, Fig. 1).

The separation into FM and AFM phases within the framework of the $t-J$ model was proposed also in Ref. [119], but without taking into account the Coulomb interaction these results may only point to a tendency toward instability of the homogeneous AFM state. Unfortunately, in Refs [97, 119] the possibility of string-like states of charge carriers was not taken into account.

Much confusion was caused by Ref. [120] which strongly influenced subsequent publications of other authors on the subject. In this study phase separation was investigated within the $t-J$ model without taking into account the Coulomb interaction. Two different explanations were proposed for this.

(1) The electrostatic fields may be compensated for by the diffusion of impurity (oxygen) ions to the regions where the charge carriers (holes) are concentrated. However, this means that the problem of the impurity metal (Sections 4.1, 4.2) should be treated, which is not the case in Ref. [120] where the electronic phase separation was treated. The interaction between impurity atoms related to incomplete compensation of the Coulomb fields of ionised impurities and holes, as well as exchange interaction between holes, were not taken into account in Ref. [120].

(2) On the other hand, Emery et al. claim that Ref. [120] is devoted to properties of the standard $t-J$ model which does not include the Coulomb interaction. However, this model was intended for the investigation of uniform states. For nonuniform states it is inadequate: any adequate model should include all substantial interactions. Otherwise, predictions of the model will have nothing in common with reality.

Mathematically, the result [120] that in a crystal a phase should arise in which each atom has lost its electron is reasonable within the framework of the model used. Such an exotic type of phase separation was obtained in the limit $|J| \gg |t|$ which also has purely mathematical meaning since, physically, J is of second order and t of the first order in the small orbital overlapping (Section 2.1). However, physically, if such a phase had formed in a real crystal, it would have exploded because of giant Coulomb forces [see (9)]. But if one tries to explain this result by the impurity phase separation, it is clear, that it might be obtained only by neglecting the interaction between impurity atoms — this interaction must prevent such a giant impurity density.

In the opposite limit the single-ferron state was rediscovered in Ref. [120]. The comments above about the ferron in the $t-J$ model are applicable to Ref. [120], too. It should only be added that the phase separation is a cooperative phenomenon, and its treatment should not be single-electron but many-electron.

After publication of Ref. [120], further development of the theory occurred along two different lines. Some authors, including the authors of Ref. [120] themselves, tried to make their results more accurate by taking into account electron-electron interaction in the nearest-neighbour approximation instead of the true Coulomb law [121, 122]. Though such an approximation is insufficient for the long-range Coulomb interaction, nevertheless, it is a step in the right direction. Already in this approximation the Coulomb repulsion hinders the phase separation. Similar qualitative results were obtained in Ref. [123] using a more complicated model. See also Ref. [124].

Other authors whose opinion of purely mathematical models is more benevolent than mine continued studying the Hubbard large-U and $t-J$ models without Coulomb interaction and constructed their phase diagrams [125–132]. In them various types of phase separation are obtained, but their phase diagrams do not always or completely coincide with the phase diagram in Ref. [120].

However, analytical results from these papers as well as from Ref. [120] confirming the existence of phase separation in these models contradict results of numerical calculations [132–134]. In particular, in Ref. [132] investigation of the 2-D Hubbard model did not lead to detection of phase separation at any values of parameters and lattice size used. It is found in Ref. [133] that the phase separation in the $t-J$ model does not occur at small J/t. This conclusion agrees with results of Ref. [134] according to which within the framework of the same model phase separation may occur only if J exceeds $4.1t$. Certainly, accounting for the Coulomb interaction would lead to still more stringent conditions for the phase separation.

The results from Ref. [132–134] just presented agree conceptually with results from Ref. [118] according to which the single-electron phase separation is absent from the $t-J$ model. It is natural to interpret them as evidence that the phase separation found in Refs [120, 125–131] is a result of the inaccurate description of the charge carriers in the models used (absence of an adequate theory for them has already been mentioned in this section).

In their most recent study [135] Emery and Kivelson claim without any proof or estimates that the Coulomb interaction should make the stationary electronic phase separation impossible. If this statement concerns only the $t-J$ model, I must agree with it and only add that it is also impossible in the absence of the Coulomb interaction. But if this statement is general then I cannot agree with it categorically. The fact that I am right is confirmed by results of numerical calculations of electronic phase separation in the $s-d$ model presented in Section 3.2. I have not seen criticism of these results by the authors of Ref. [135].

Their correctness is confirmed by the experiment described in Sections 3.4, 3.5.

Instead of a stationary phase separation, Emery and Kivelson have postulated in Ref. [135] a fluctuating phase separation. As proof of the existence of this phenomenon is not given in Ref. [135], there is no reason for its discussion in the present review.

So far the standard $t-J$ model with interaction only between the first neighbouring atoms was under discussion. In a generalised $t-J$ model with frustrated exchange interaction ($t-J-J'$ model) phase separation is theoretically possible but it occurs as a result of the transition from the initial phase to the changed phase not of conduction electrons or holes but of strings [136].

The string energy in a 2-D Ising antiferromagnetic system with stripe ordering with $\boldsymbol{Q} = (\pi, 0)$ turns out to be lower than with staggered ordering with $\boldsymbol{Q} = (\pi, \pi)$ for the following reason. As was already indicated, while moving throughout the antiferromagnetic structure, the electron leaves a chain of reversed spins along its path. This chain corresponds to the antiphase ordering along the path (Fig. 16). If the electron moves throughout the staggered structure, then its transition to the nearest neighbour (but not backwards) is accompanied by the appearance of reversed spin on the atom which it leaves. But in the case of stripe ordering, spin reversal does not occur when the electron moves along the FM 'layers'. Thus, at equal separations from the string equilibrium position, the average number of reversed spins for staggered ordering is larger than for stripe ordering. Respectively, in the first case the direct exchange energy, approximately proportional to the number of reversed spins, turns out to be higher than in the second case.

As in the case of the afmon (Section 2.4), it will be assumed that in the absence of the charge carriers the staggered phase has a lower energy than the stripe phase, but the difference of their direct exchange energies $D = 2J_2 - J_1$ is very small. Then the string self-trapping inside a region of the stripe phase leads to a gain in the energy of the order of F/b. Here $F \propto J_2/a$ is the 'elastic' force of exchange origin which acts upon the charge carrier oscillating about its equilibrium point. The quantity $1/b \propto |t/J_2|^{1/3}a$ is the amplitude of string oscillation.

The estimate above only points to the possibility of single-electron phase separation according to the string mechanism (conceptually, this is double self-trapping: the first self-trapping is the string formation and the second self-trapping is the string transition to another phase). To prove the possibility of phase separation in a degenerate semiconductor according to a similar mechanism, it is necessary to consider the many-string problem with allowance for the Coulomb interaction.

5.4 Electronic and impurity phase separation in quasi-two-dimensional systems described by the $s-d$ model

In this section a generalisation of the theory of electronic and impurity phase separation in the $s-d$ model (Sections 3.1–3.3 and 4.2–4.3) to the quasi-two-dimensional systems of HTSC type [137] will be put forward. A crystal is considered which consists of crystallographic planes which do not permit electron hoppings between them. Analysis carried out in Ref. [137] suggests that at the electronic phase separation the most energetically favoured geometry corresponds to a crystal consisting of a set of plane-parallel sandwiches. The central position in each sandwich is occupied by a plane with a changed magnetic ordering in which all the charge carriers of this sandwich are concentrated. On both sides of the central plane, no-charge-carrier planes in the initial magnetic state are located. Each such sandwich is electroneutral as a whole. If one neglects the anisotropy of the dielectric constant for the sake of simplicity and uses the same variational parameter x (the ratio of volumes of the initial and newly-arising phases), one may easily find the following expression for the energy of the system per charge carrier:

$$H = \frac{E}{N_e} = \chi\pi n(1+x)\,\frac{a}{m} + \frac{D}{\nu(1+x)} - U + \frac{\pi}{6}\,x^2 e^2 a^2\,\frac{n(1+x)}{\varepsilon}\,, \tag{27}$$

where χ is equal to 1 for the FM ordering and to 0.5 for nonmagnetised ordering in the changed magnetic phase, $\nu = na^3$. If one neglects the Coulomb interaction, then minimisation of Eqn (27) with respect to x makes it possible to find explicit expressions for equilibrium values of H and x:

$$x = -1 + \frac{1}{\nu}\left(\frac{Dma^2}{\pi\chi}\right)^{1/2}, \tag{28}$$

$$H = 2\left(\frac{\pi\chi D}{a^2 m}\right)^{1/2} - U\,. \tag{29}$$

As seen from Eqn (29), in the limit $\varepsilon \Rightarrow \infty$ the self-trapping energy H does not depend on the electron density ν. The condition for cooperative self-trapping following from Eqn (29) is much more favourable than condition (5) for single-electron self-trapping: at $\chi = 1$ the critical value U_c for the depth of the potential well is in the former case 1.55 times lower than in the latter case, amounting to less than 0.5 eV at $D = 0.1$ eV. Such U values are quite realistic for HTSCs.

Numerical calculations show that the Coulomb interaction drastically increases the energy of a system with such a geometry only at the smallest ν values which means that the single-electron self-trapping becomes the most energetically favoured. But with increasing ν the role of the Coulomb interaction is sharply reduced. For example, at $\varepsilon = 10$ and $D = 0.1$ eV the quantity U_c diminishes from 1.695 eV at $\nu = 0.01$ ($x = 7.51$) to 0.604 eV at $\nu = 0.13$ ($x = 0.9$).

The Coulomb effects are suppressed at the impurity phase separation. Unlike the impurity phase separation in nonmagnetic semiconductors, in magnetic semiconductors it is driven not only by interaction between impurity atoms but also by reduction of the impurity-atom energy at formation of a new magnetic phase. In what follows, an expression will be written down for the energy of the quasi-two-dimensional impurity metal in the model already used which is similar to Eqns (17), (20) [137]. It will be refined by comparison with the jellium model to which these equations correspond: the Coulomb interaction between charge carriers and ionised impurity will be described more accurately. Namely, only the charge of the former will be assumed to be distributed uniformly over the crystal, and the energy of their interaction by point charges of ions will be found with the use of Wigner spheres.

The exchange energy is calculated by the use of two-dimensional plane waves as single-electron states, and the correlation energy is not taken into account. Then one obtains for the energy of the impurity metal ($\sigma = na$)

$$\lambda = \frac{E}{N} = \frac{2\pi\sigma\chi}{m} - 4\pi^{1/2} G \frac{e^2}{\varepsilon} \sigma^{1/2} \chi^{1/2} - 0.9 \left(\frac{4\pi}{3}\right)^{1/3} \frac{e^2}{\varepsilon} \left(\frac{\sigma}{a}\right)^{1/3}, \quad G \approx 0.4 \,. \tag{30}$$

Expressions (30), one of which, similarly to (19), is supplemented by the energy of formation of the new phase and the energy of charge carriers in it, are substituted in Eqns (23), (24). From them conditions are found for the coexistence of two different magnetic phases with two different impurity densities. Such a situation may exist if the set of equations obtained has physically reasonable solutions σ_1 and σ_2 for optimal two-dimensional impurity densities in both phases $a^{-2} \gg \sigma_1 > \sigma_2 > 0$. Then in the σ range between σ_1 and σ_2 both phases 1 and 2 may coexist, their relative volumes being correspondingly $(\sigma - \sigma_2)/(\sigma_1 - \sigma_2)$ and $(\sigma_1 - \sigma)/(\sigma_1 - \sigma_2)$.

Numerical estimates of realistic values of parameters show that such a situation may exist. This means that two different magnetic phases with different impurity densities, i.e. two different types of impurity metal, may coexist. One of these phases or even both may be superconducting.

If nontrivial solutions of Eqns (23), (24) and (30) do not exist, then all the impurity is concentrated in one of the phases, and the other phase is insulating. The volumes of the high-conducting and insulating phases should be found from the condition of minimum total energy.

6. Conclusion

It follows from the above that the thermodynamic-equilibrium phase separation is typical of such materials as degenerate magnetic semiconductors and magnetic-semiconductor-based high-temperature superconductors. One should distinguish two types of phase separation: the electronic one occurring at a frozen impurity and for this reason in equilibrium only with respect to the charge carriers and magnetic subsystem, and the impurity one which is in equilibrium with respect to the impurity atom positions, too.

The electronic phase separation occurs by the following mechanism: the charge carriers create regions of a new magnetic phase which is normally unstable in this crystal. But in this phase the carrier energy is lower than in the initial phase. The carriers make the new phase stable by means of their concentration inside it. The regions of the initial phase do not contain carriers and for this reason are insulating. If the initial phase is antiferromagnetic, then the new phase may be ferromagnetic, antiferromagnetic with another type of ordering, magnetically disordered, and so on.

As the phase separation is accompanied by the charge separation here, the Coulomb forces cause phase intermixing. The detailed geometry of a two-phase state depends on the charge carrier density and crystallographic anisotropy. At relatively small densities in an isotropic crystal, high-conducting droplets of the new phase form an almost-periodic structure inside the insulating initial phase. Then, as a whole, the crystal behaves like an insulator. But, on increase in the electron density, the portion of the new phase increases, and the electron droplets begin to make contact with each other. As a result, percolation of the electron liquid and of the new phase occurs.

The electronically-nonuniform phase-separated state is the crystal ground state and resembles, to some extent, the Wigner crystal or a nonlinear superposition of charge density waves and spin density waves. It was observed experimentally in EuSe, EuTe and other antiferromagnetic crystals. In highly-anisotropic crystals of the HTSC type the two-phase state is characterised by a plane geometry. The electronic phase separation is likely to exist in some HTSCs.

The impurity phase separation in the materials considered is driven simultaneously by interaction between the impurity atoms, which tends to establish an optimal separation between them, and by their tendency to establish a magnetic ordering at which their energy is minimal (in this respect they behave like charge carriers). As a result, the impurity turns out to be distributed nonuniformly over the crystal, and this may be accompanied by the appearance of different magnetic phases in regions with enhanced and reduced impurity densities. However, there is no mutual phase charging or related effects. Impurity phase separation was observed experimentally both in some nonsuperconducting semiconductors and in some high-temperature superconductors.

The phase separation by itself is not directly related to the superconductivity since it occurs in nonsuperconducting materials, and in superconductors it occurs at temperatures considerably higher than the superconducting transition temperature. In addition, in many superconductors it was not observed at all. However, phase separation favours superconductivity and creates optimal conditions for it.

References

1. Nagaev E L *Pis'ma Zh. Eksp. Teor. Fiz.* **6** 484 (1967) [*JETP Lett.* **6** 18 (1967)]
2. Nagaev E L *Zh. Eksp. Teor. Fiz.* **54** 228 (1968) [*Sov. Phys. Lett.* **27** 122 (1968)]
3. Nagaev E L *Pis'ma Zh. Eksp. Teor. Fiz.* **16** 558 (1972) [*JETP Lett.* **16** 394 (1972)]
4. Kashin V A, Nagaev E L *Zh. Eksp. Teor. Fiz.* **66** 2105 (1974) [*Sov. Phys. JETP* **39** 1036 (1974)]
5. Lazarev G L, Matveev V M, Nagaev E L *Fiz. Tverd. Tela* **17** 1955 (1975) [*Sov. Phys. Solid State* **17** 1280 (1975)]
6. Nagaev E L *Pis'ma Zh. Eksp. Teor. Fiz.* **55** 646 (1992) [*JETP Lett.* **55** 675 (1992)]
7. Nagaev E L *Phys. Lett. A* **170** 454 (1992)
8. Nagaev E L *Zh. Eksp. Teor. Fiz.* **104** 2483 (1993) [*J. Exp. Theor. Phys.* **77** 118 (1993)]
9. Nagaev E L *Physics of Magnetic Semiconductors* (Moscow: Mir, 1983)
10. Nagaev E L, Podel'shchikov A I *Zh. Eksp. Teor. Fiz.* **98** 1972 (1990) [*Sov. Phys. JETP* **71** 1108 (1990)]
11. Nagaev E L, Podel'shchikov A I *Phys. Lett. A* **144** 473 (1990)
12. Nagaev E L *J. Magn. Magn. Mat.* **110** 39 (1992)
13. Nagaev E L, Podel'shchikov A I *Physica C* **205** 91 (1993); Nagaev E L *Zh. Eksp. Teor. Fiz.* **103** 252 (1993) [*J. Exp. Theor. Phys.* **76** 138 (1993)]
14. Vitins J, Wachter P *Phys. Rev. B* **12** 3829 (1975)
15. Vitins J, Wachter P *Solid State Commun.* **33** 1273 (1977)
16. Oliveira Jr N, Foner S, Shapira Y, Reed T *Phys. Rev. B* **5** 2634 (1972)
17. Shapira Y, Foner S, Oliveira Jr N, Reed T *Phys. Rev. B* **5** 2674 (1972)
18. Shapira Y, Foner S, Oliveira Jr N *Phys. Rev. B* **10** 4765 (1974)

19. Vitins J, Wachter P *Proc. Intern. Conf. on Magnetism* (Moscow, 1973) vol. 1, p. 140
20. Gor'kov L P, Sokov A V *Pis'ma Zh. Eksp. Teor. Fiz.* **46** 333 (1987) [*JETP Lett.* **46** 420 (1987)]
21. Gorbatsevich A A, Kopaev Yu V, Tokatly I V *Pis'ma Zh. Eksp. Teor. Fiz.* **52** 736 (1990) [*JETP Lett.* **52** 95 (1990)]
22. Gorbatsevich A A, Kopaev Yu V, Tokatly I V *Zh. Eksp. Teor. Fiz.* **101** 971 (1992) [*Sov. Phys. JETP* **74** 521 (1992)]
23. Kastalskii A A, Maltsev S B *Solid State Commun.* **17** 107 (1975)
24. Vengalis B Yu, Kastalskii A A, Mal'tsev S B *Pis'ma Zh. Eksp. Teor. Fiz.* **22** 7 (1975) [*JETP Lett.* **22** 3 (1975)]
25. Vengalis B, Kastalskii A *Solid State Commun.* **30** 13 (1979)
26. Vengalis B U, Kastalskii A A *Fiz. Tverd. Tela* **20** 2753 1978 [*Sov. Phys. Solid State.* **20** 1588 (1978)]
27. Rose Jr J H, Shore H B, Zaremba E *Phys. Rev. Lett.* **37** 354 (1976)
28. Roitburt A L *Usp. Fiz. Nauk* **113** 69 (1974) [*Sov. Phys. Usp.* **17** 326 (1974)]
29. Khachaturyan A G *Teoriya Fazovykh Prevrashchenii i Struktura Tverdykh Rastvorov* (Theory of Phase Transformations and the Structure of Solid Solutions) (Moscow: Nauka, 1974)
30. Nagaev E L *Physica C* **222** 324 (1994)
31. Zhang W, Bennemann K *Phys. Rev. B* **45** 12487 (1992)
32. Krivoglaz M A *Usp. Fiz. Nauk* **111** 617 (1973) [*Sov. Phys. Usp.* **16** 856 (1974)]
33. Nagaev E L, Podel'shchikov A I *Fiz. Tverd. Tela* **23** 859 (1981) [*Sov. Phys. Solid State* **23** 487 (1981)]
34. Nagaev E L *Usp. Fiz. Nauk* **117** 437 (1975) [*Sov. Phys. Usp.* **18** 863 (1975)]
35. Mott N, Zinamon Z *Rep. Prog. Phys.* **33** 881 (1970)
36. Pokrovskii V L, Uimin G V, Khvoshchenko D V *Pis'ma Zh. Eksp. Teor. Fiz.* **46** Suppl. 136 (1987) [*JETP Lett. Suppl.* **46** S113 (1987)]
37. Lakhno V D, Nagaev E L *Fiz. Tverd. Tela* **18** 259 (1976) [*Sov. Phys. Solid State* **18** 151 (1976)]
38. Nagaev E L , Podel'shchikov A I *Fiz. Tverd. Tela.* **24** 3033 (1982) [*Sov. Phys. Solid State* **24** 1717 (1982)]
39. Lakhno V D, Nagaev E L *Fiz. Tverd. Tela* **20** 82 (1978) [*Sov. Phys. Solid State* **20** 44 (1978)]
40. Koroleva L I, Nagaev E L, Tsvetkova N A *Zh. Eksp. Teor. Fiz.* **79** 600 (1980) [*Sov. Phys. JETP* **52** 303 (1980)]
41. Kozintseva M B, Zil'berwarg V E *Phys. Status Solidi B* **74** 199 (1976)
42. Wood R, Mostoller M, Cooke J *Physica C* **165** 97 (1990)
43. Wood R, Abdel-Raouf M *Solid State Commun.* **74** 371 (1990)
44. Wood R *Phys. Rev. Lett.* **66** 829 (1991)
45. Wood R, Cooke J *Phys. Rev. B* **45** 5585 (1992)
46. Sabczynski J, Schreiber M, Scherman A *Phys. Rev. B* **48** 543 (1993)
47. Pokrovskii V L, Uimin G V *Physica C* **160** 323 (1989)
48. Aharony A *Phys. Rev. Lett.* **60** 1330 (1988)
49. Koroleva L I, Odintsov A G, Mashaev M Kh, Saifullaeva D A *Pis'ma Zh. Eksp. Teor. Fiz.* **57** 793 (1993) [*JETP Lett.* **57** 808 (1993)]
50. Nagaev E L *Pis'ma Zh. Eksp. Teor. Fiz.* **25** 87 (1977) [*JETP Lett.* **25** 76 (1977)]
51. Koroleva L A, Shalimova M A *Fiz. Tverd. Tela* **21** 449 (1979) [*Sov. Phys. Solid State* **21** 266 (1979)]
52. Nagaev E L *Zh. Eksp. Teor. Fiz.* **59** 1215 (1970) [*Sov. Phys. JETP* **32** 664 (1971)]
53. Zatsarinnii O I, Nagaev E L *Pis'ma Zh. Eksp. Teor. Fiz.* **25** 505 (1977) [*JETP Lett.* **25** 475 (1977)]
54. Nagaev E L, Podel'shchikov A I *Zh. Eksp. Teor. Fiz.* **86** 1831 (1984) [*Sov. Phys. JETP* **59** 1065 (1984)]
55. Nagaev E L, Podel'shchikov A I *Zh. Eksp. Teor. Fiz.* **104** 3643 (1993) [*J. Exp. Theor. Phys.* **77** 739 (1993)]
56. Visscher P *Phys. Rev. B* **10** 943 (1974)
57. Auslender M I, Katsnelson M I *Solid State Commun.* **44** 387 (1982)
58. Andreev A F *Pis'ma Zh. Eksp. Teor. Fiz.* **24** 608 (1976) [*JETP Lett.* **24** 564 (1976)]
59. Paradishvili I N *Pis'ma Zh. Eksp. Teor. Fiz.* **28** 276 (1978) [*JETP Lett.* **28** 252 (1978)]
60. Pushkarov D I *Pis'ma Zh. Eksp. Teor. Fiz.* **27** 359 (1978) [*JETP Lett.* **27** 337 (1978)]
61. Feigel'man M V *Pis'ma Zh. Eksp. Teor. Fiz.* **27** 491 (1978) [*JETP Lett.* **27** 462 (1978)]
62. Umehara M *J. Magn. Magn. Mat.* **52** 406 (1985)
63. Umehara M *Phys. Rev. B* **36** 574 (1987)
64. Umehara M *Phys. Rev. B* **39** 7101 (1989)
65. Umehara M *Phys. Rev. B* **41** 2421 (1990)
66. Kasuya T *Solid State Commun.* **18** 51 (1976)
67. Nagaev E L *Phys. Rep.* **222** 201 (1992)
68. Gaeta G *Phys. Lett. A* **148** 98 (1990)
69. Nagaev E L, Sokolova E B *Fiz. Tverd. Tela* **21** 1326 (1979) [*Sov. Phys. Solid State* **21** 767 (1979)]
70. Osipov V V, Kochev I V *Fiz. Tverd. Tela* **33** 942 (1991) [*Sov. Phys. Solid State* **33** 535 (1991)]
71. Osipov V V, Samokhvalov A A, Nagaev E L *Z. Phys. B* **96** 31 (1994)
72. Bonch-Bruevich V L, Zvyagin I P, Mironov A G *Domennaya Electricheskaya Neustoichivost' v Poluprovodnikakh* (Domain Electric Instability in Semiconductors) (Moscow: Nauka, 1972)
73. Andrianov D G, Drozdov S A, Lazareva G V *Fiz. Nizk. Temp.* **3** 497 (1977) [*Sov. J. Low Temp. Phys.* **3** 241 (1977)]
74. Kamijo A, Katase A, Isikawa Y *J. Phys. Colloq.* **41** 5 (1980)
75. Wachter P, Kaldis E *Solid State Commun.* **34** 241 (1980)
76. Hammel P, Reyes A, Cheong S-W et al. *Phys. Rev. Lett.* **71** 440 (1993)
77. Hirakawa J *J. Phys. Soc. Jpn.* **15** 2063 (1960)
78. Wollan E, Koehler W *Phys. Rev.* **100** 545 (1955)
79. Jonker C, Van Santen J *Physica* **160** 337 (1950); **19** 120 (1953)
80. Tamura S, Kuriyama M *Phys. Lett. A* **70** 469 (1979)
81. Tamura S *Phys. Lett. A* **78** 401 (1980)
82. Izyumov Yu A, Ozerov R P *Magnitnaya Neitronografiya* (Magnetic Neutronography) (Moscow: Nauka, 1966)
83. Volger J *Physica* **20** 49 (1954)
84. Troyanchuk I O *Zh. Eksp. Teor. Fiz.* **102** 251 (1992) [*Sov. Phys. JETP* **75** 132 (1992)]
85. Bednorz J, Mueller K *Z. Phys. B* **64** 189 (1986)
86. Mueller K, Takashige H, Bednorz J *Phys. Rev. Lett.* **58** 1143 (1987)
87. Jorgensen J, Dabrovski B, Pei S et al. *Phys. Rev. B* **38** 11337 (1988)
88. Dabrowsky B, Jorgensen J, Hinks D et al. *Physica* **162–164** 99 (1989)
89. Chaillout C, Chenavas J, Cheong S et al. *Physica C* **170** 87 (1990)
90. Ueda K, Sugata T, Kohara Y et al. *Solid State Commun.* **73** 49 (1990);
Kobayashi T, Wada S, Shibutani K, Ogawa K *J. Phys. Soc. Jpn.* **58** 3497 (1989)
91. Hammel P, Reyes A, Fisk Z et al. *Phys. Rev. B* **42** 6781 (1990)
92. Ryder J, Midgley P, Exley R et al. *Physica C* **173** 9 (1991);
Hundley M, Thompson J, Cheong S-W et al. *Phys. Rev. B* **47** 4062 (1990)
93. Cho J, Chou F, Johnston D *Phys. Rev. Lett.* **70** 222 (1993)
94. Weidinger A, Niedermayer C, Golnik A et al. *Phys. Rev. Lett.* **62** 102 (1989)
95. Thio T, Thurston T, Preyer N et al. *Phys. Rev. B* **38** 905 (1988)
96. Kremer R, Sigmund E, Hizhnyakov V et al. *Z. Phys. B* **86** 319 (1992);
Kremer R, Hizhnyakov V, Sigmund E et al. *Z. Phys. B* **91** 169 (1993)
97. Hizhnyakov V, Sigmund E *Physica C* **156** 655 (1988);
Hizhnyakov V, Kristoffel N, Sigmund E *Physica C* **161** 435 (1989);
Hizhnyakov V, Sigmund E, Zavt G *Phys. Rev. B* **44** 12639 (1991); Seibold G, Sigmund E, Hizhnyakov V *Phys. Rev. B* **48** 7537 (1993)
98. Mehring M, in *Phase Separation in Cuprate Superconductors* (Eds K Mueller, G Benedek) (Singapore: World Scientific, 1992); Wuebbeler G, Schirmer O *Phys. Status Solidi B* **174** K21 (1992)

99. Zakharov A A, Nikonov A A, Parfionov O E et al. *Physica C* **223** 157 (1994)
100. Osofsky M, Cohn J, Skelton E et al. *Phys. Rev. B* **45** 4916 (1992)
101. Cava R, Hewat A, Hewat E *Physica C* **165** 419 (1990)
102. Hodges J, Bonville P, Imbert P et al. *Physica C* **184** 270 (1991)
103. Yu G, Heeger A, Stucky G et al. *Solid State Commun.* **72** 345 (1992)
104. Yu G, Lee C, Heeger A et al. *Phys. Rev. Lett.* **67** 2581 (1991)
105. Yu G, Lee C, Heeger A et al. *Physica C* **190** 563 (1992)
106. Bulaevskii L N, Panyukov S V, Sadovskii M V *Zh. Eksp. Teor. Fiz.* **92** 672 (1987) [*Sov. Phys. JETP* **65** 380 (1987)]
107. Kovalenko V F, Nagaev E L *Usp. Fiz. Nauk* **148** 561 (1986) [*Sov. Phys. Usp.* **29** 297 (1986)]
108. Nagaev E L *Phys. Status Solidi B* **145** 11 (1988)
109. Mesot J, Allenspach P, Staub U et al. *Phys. Rev. Lett.* **70** 865 (1993)
110. Radaelli P, Segre C, Hinks D, Jorgensen J *Phys. Rev. B* **45** 4923 (1992)
111. Chechersky V, Kopelev N, Beom-hoan O et al. *Phys. Rev. Lett.* **70** 3355 (1993)
112. Reddy P, Ramma Y *Solid State Commun.* **74** 377 (1990)
113. Senaris-Rodrigues M, Garcia-Alvarado F, Moran E et al. *Physica C* **162–164** 85 (1989)
114. Anshukova N V, Ginodman V B, Golovashkin A I et al. *Zh. Eksp. Teor. Fiz.* **97** 1635 (1990) [*Sov. Phys. JETP* **70** 923 (1990)]
115. Aligia A, Balina M *Phys. Rev. B* **47** 14380 (1993)
116. Bulaevskii L N, Nagaev E L, Khomskii D I *Zh. Eksp. Teor. Fiz.* **54** 1562 (1968) [*Sov. Phys. JETP* **27** 836 (1968)]
117. Nagaev E L *Zh. Eksp. Teor. Fiz.* **58** 1269 (1970) [*Sov. Phys. JETP* **31** 682 (1970)]
118. Nagaev E L *Zh. Eksp. Teor. Fiz.* **100** 961 (1991) [*Sov. Phys. JETP* **73** 530 (1991)]
119. Marder M, Papanicolaou N, Psaltakis G *Phys. Rev. B* **41** 6920 (1990)
120. Emery V, Kivelson S, Lin H *Phys. Rev. Lett.* **64** 475 (1990)
121. Kivelson S, Emery V, Lin H *Phys. Rev. B* **42** 6523 (1990)
122. Fehske H, Waas V, Roder H *Solid State Commun.* **76** 1333 (1990)
123. Uhrig G, Vlaming R *Phys. Rev. Lett.* **71** 371 (1993)
124. Sudbo A, Schmitt-Rink S, Varma C *Phys. Rev. B* **46** 5548 (1992)
125. Krivnov V, Ovchinnikov A *Phys. Rev. B* **45** 12996 (1992)
126. Angelucci A, Sorella S *Phys. Rev. B* **47** 8858 (1993)
127. Putikka W, Luchini M, Rice T *Phys. Rev. Lett.* **68** 538 (1992)
128. Singh A, Tesanovich Z, Kim J *Phys. Rev. B* **44** 7757 (1991)
129. Carstensen J, Dichtel K *Phys. Rev. B* **46** 11040 (1992)
130. Shiping Feng *J. Phys. C* **5** 115 (1993)
131. Bang Y, Kotliar G, Castellano C et al. *Phys. Rev. B* **43** 13724 (1991)
132. Moreo A, Scalapino D, Dagotto E *Phys. Rev. B* **43** 11442 (1991)
133. Dagotto E, Moreo A, Ortolani F et al. *Phys. Rev. B* **45** 10741 (1992)
134. Waas V, Fehske H, Buettner H *Phys. Rev. B* **48** 9106 (1993)
135. Emery V, Kivelson S *Physica C* **209** 597 (1993)
136. Nagaev E L *Phys. Lett. A* **184** 297 (1994)
137. Nagaev E L *Z. Phys. B* (in press)